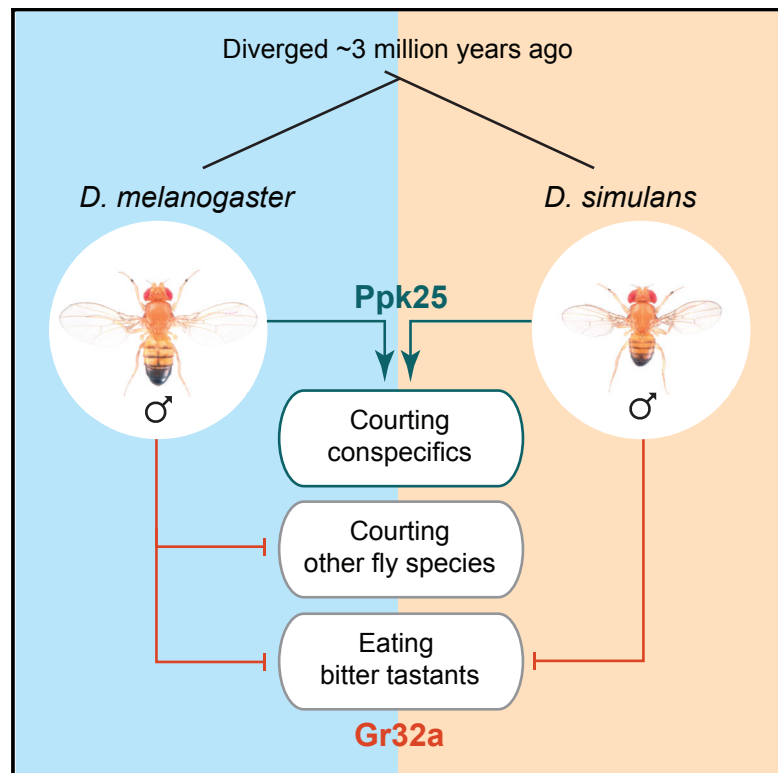# Evolution of Mechanisms that Control Mating in *Drosophila* Males

Graphical Abstract

Authors

Osama M. Ahmed, Aram Avila-Herrera, Khin May Tun, ..., Graeme W. Davis, Katherine S. Pollard, Nirao M. Shah

Correspondence

nirao@stanford.edu

In Brief

Mechanisms that inhibit interspecies mating are critical to reproductive isolation of species. Ahmed et al. show that Gr32a, a chemoreceptor that inhibits interspecies courtship by *D. melanogaster* males, does not inhibit this behavior in the closely related *D. simulans*, indicating rapid evolution of peripheral sensory mechanisms that preclude interspecies breeding.

Highlights

- Gr32a and Gr33a do not inhibit interspecies or intermale mating by male *D. simulans*

- Gr32a and Gr33a inhibit feeding of bitter tastants by *D. simulans*

- Ppk25 promotes mating with conspecific females by male *D. simulans*

- Pathways that promote or inhibit mating have evolved differentially in *D. simulans*

CellPress

Evolution of Mechanisms that Control Mating in *Drosophila* Males

Osama M. Ahmed,[3,9] Aram Avila-Herrera,[4,10,11] Khin May Tun,[5] Paula H. Serpa,[4] Justin Peng,[4] Srinivas Parthasarathy,[1,12] Jon-Michael Knapp,[2,13] David L. Stern,[13] Graeme W. Davis,[8] Katherine S. Pollard,[6,7,11] and Nirao M. Shah[1,2,5,14,*]

[1]Department of Psychiatry and Behavioral Sciences, Stanford University, Stanford, CA 94305, USA
[2]Department of Neurobiology, Stanford University, Stanford, CA 94305, USA
[3]Program in Neuroscience, University of California, San Francisco, San Francisco, CA 94143, USA
[4]Integrative Program in Quantitative Biology, University of California, San Francisco, San Francisco, CA 94158, USA
[5]Department of Anatomy, University of California, San Francisco, San Francisco, CA 94143, USA
[6]Institute for Human Genetics, University of California, San Francisco, San Francisco, CA 94143, USA
[7]Department of Epidemiology and Biostatistics, University of California, San Francisco, San Francisco, CA 94158, USA
[8]Department of Biochemistry and Biophysics, University of California, San Francisco, San Francisco, CA 94158, USA
[9]Princeton Neuroscience Institute, Princeton University, Princeton, NJ 08540, USA
[10]Computation Directorate, Lawrence Livermore National Laboratory, Livermore, CA 94550, USA
[11]Gladstone Institutes, San Francisco, CA 94158, USA
[12]L.E.K. Consulting, 75 State Street, Boston, MA 02109, USA
[13]Janelia Research Campus, HHMI Ashburn, Ashburn, VA 20147, USA
[14]Lead Contact
*Correspondence: nirao@stanford.edu
https://doi.org/10.1016/j.celrep.2019.04.104

SUMMARY

Genetically wired neural mechanisms inhibit mating between species because even naive animals rarely mate with other species. These mechanisms can evolve through changes in expression or function of key genes in sensory pathways or central circuits. Gr32a is a gustatory chemoreceptor that, in *D. melanogaster*, is essential to inhibit interspecies courtship and sense quinine. Similar to *D. melanogaster*, we find that *D. simulans* Gr32a is expressed in foreleg tarsi, sensorimotor appendages that inhibit interspecies courtship, and it is required to sense quinine. Nevertheless, Gr32a is not required to inhibit interspecies mating by *D. simulans* males. However, and similar to its function in *D. melanogaster*, Ppk25, a member of the Pickpocket family, promotes conspecific courtship in *D. simulans*. Together, we have identified distinct evolutionary mechanisms underlying chemosensory control of taste and courtship in closely related *Drosophila* species.

INTRODUCTION

A species can be defined as a set of organisms that share a gene pool and breed with one another (Darwin, 1860; Dobzhansky, 1937; Mayr, 1988). The lack of interspecies breeding preserves advantages conferred by species-specific allele combinations (Mayr, 1988; Mayr and Dobzhansky, 1945; Orr, 2005; Orr et al., 2004), and mechanisms that preclude interbreeding must evolve rapidly to facilitate reproductive isolation between closely related species (Coyne and Orr, 1989; Mendelson, 2003). Individuals from closely related species rarely attempt to mate, suggesting that neural pathways underlying behavioral barriers to interbreeding must also evolve rapidly. How such neural pathways evolve is poorly understood.

Drosophilids provide a facile model for studies on how neural pathways have evolved. There are ~1,500 drosophilid species, many of which co-exist in overlapping habitats (Jezovit et al., 2017; Markow, 2015). They engage in species-typical stereotyped courtship rituals, and many genetic and neural pathways that regulate courtship of *D. melanogaster* are well defined (Bastock and Manning, 1955; Clowney et al., 2015; Demir and Dickson, 2005; Gill, 1963; Greenspan and Ferveur, 2000; Hall, 1978, 1994; Hotta and Benzer, 1976; Kallman et al., 2015; Kohatsu et al., 2011; Lin et al., 2016; Manoli et al., 2005; Pavlou and Goodwin, 2013; Ryner et al., 1996; Spieth, 1952; Thistle et al., 2012; Tootoonian et al., 2012). We previously demonstrated that sensory neurons expressing the gustatory chemoreceptor Gr32a are necessary to suppress interspecies courtship by *D. melanogaster* males (Fan et al., 2013). In addition, Gr32a is required to recognize cuticular hydrocarbons on non-*melanogaster* drosophilids and to inhibit interspecies mating. Strikingly, Gr32a is also necessary to inhibit courtship displays toward the closely related *D. simulans*, which last shared an ancestor with *D. melanogaster* ~3 million to 5 million years ago (mya) (David et al., 2007; Tamura et al., 2004). *D. simulans* and *D. melanogaster* co-exist globally (reviewed in Jezovit et al., 2017) and are very similar in behavior and appearance (Sturtevant, 1919, 1920). Here we have examined how the Gr32a chemosensory pathway has evolved to inhibit interspecies courtship in *D. simulans*.
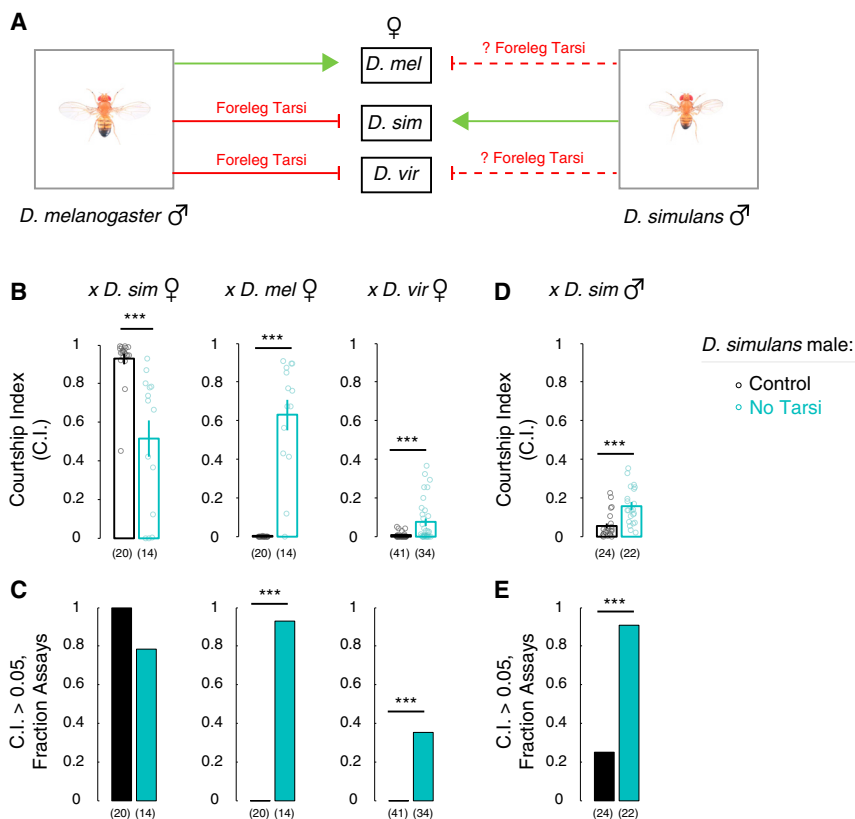
Figure 1. *D. simulans* Male Foreleg Tarsi Inhibit Courtship of Other Species and Are Not Essential for Courtship of Conspecific Females

(A) We tested whether, similar to *D. melanogaster* males, foreleg tarsi also inhibited interspecies courtship by *D. simulans* males.

(B) *D. simulans* males lacking foreleg tarsi court conspecific, *D. melanogaster*, and *D. virilis* females.

(C) *D. simulans* males lacking foreleg tarsi are more likely to show intense courtship toward *D. melanogaster* and *D. virilis* females.

(D) *D. simulans* males lacking foreleg tarsi show more courtship toward conspecific males.

(E) *D. simulans* males lacking foreleg tarsi are more likely to show intense courtship toward conspecific males.

Mean ± SEM. CI, fraction time spent courting target fly. Each circle denotes CI of one male. n = 14–41 per cohort. ***p < 0.001. See also Figure S1.

RESULTS

The Chemosensory Pathway that Inhibits Interspecies Courtship Is Conserved

D. melanogaster males tap potential mates with their foreleg tarsi very early in courtship. This tapping restricts courtship to conspecifics because males lacking foreleg tarsi court conspecifics as well as other drosophilid species (Figure 1A) (Fan et al., 2013; Manning, 1959; Spieth, 1952). Similarly, *D. simulans* males also tap potential mates with foreleg tarsi (Manning, 1959; Spieth, 1952), and surgical extirpation of these tarsi enables *D. simulans* males to court *D. melanogaster* females (Fan et al., 2013; Manning, 1959; Spieth, 1952). We found that tarsiless *D. simulans* males also courted *D. virilis* females, a distantly related drosophilid (shared last common ancestor ∼40 mya), and conspecific males (Figures 1B–1E and S1A). Tarsiless *D. simulans* males, like their *D. melanogaster* counterparts (Fan et al., 2013), also courted conspecific females (Figures 1B and 1C). Such conspecific courtship was performed by the tarsiless males at reduced intensity, likely because of reduced effectiveness in pursuing females or from loss of tarsal neurons that promote courtship. However, loss of tarsi did not lead to overall reduction in locomotor activity during conspecific courtship (Figure S1I); tarsiless males did show a small increase in locomotor activity when paired with *D. melanogaster* females (Figure S1J), most likely because they persisted in courting the females despite being rejected. Regardless, tarsiless

D. simulans males, similar to their *D. melanogaster* counterparts, courted other species.

The hydrocarbon 7-tricosene is enriched on the cuticle of *D. simulans* females and depleted on the cuticle of *D. melanogaster* females, and it serves as an aphrodisiac and repellent, respectively, for *D. simulans* and *D. melanogaster* males (Billeter et al., 2009; Coyne et al., 1994; Everaerts et al., 2010; Fan et al., 2013; Ferveur, 2005; Jallon, 1984; Lacaille et al., 2007; Wang et al., 2011). Accordingly, wild-type (WT) *D. simulans* courted *D. yakuba* females, whose cuticle is enriched in 7-tricosene, albeit with lower intensity compared with conspecific females (p < 0.001, n = 20–22 males/cohort; see Figures S1B and 1B). Tarsectomy of males did not further increase courtship toward *D. yakuba* females (Figure S1B), suggesting that multiple pathways exist in *D. simulans* to inhibit interspecies courtship. Nevertheless, severing foreleg tarsi of *D. simulans* males disinhibits courtship toward other species without abolishing courtship with conspecific females.

Gr32a Expression Is Conserved in *D. simulans* Foreleg Tarsi

Gr32a is expressed in sensory neurons in distal foreleg tarsi of *D. melanogaster* (Koganezawa et al., 2010; Miyamoto and Amrein, 2008; Moon et al., 2009; Scott et al., 2001; Thistle et al., 2012; Thorne et al., 2004), and it is required to detect contact-dependent cues on other species and to inhibit interspecies courtship (Fan et al., 2013) (Figure 2A). The genome of *D. simulans* encodes an ortholog of *Gr32a* (Drosophila 12 Genomes Consortium et al., 2007) (with four coding exons in both species and 97.8% identity in the encoded protein; Data S1), and we wondered whether this gene is expressed in foreleg tarsi of this species. The ∼3.8 kb of *D. melanogaster* genomic DNA 5′ of the start codon is sufficient to drive reporter expression in subsets of neurons in
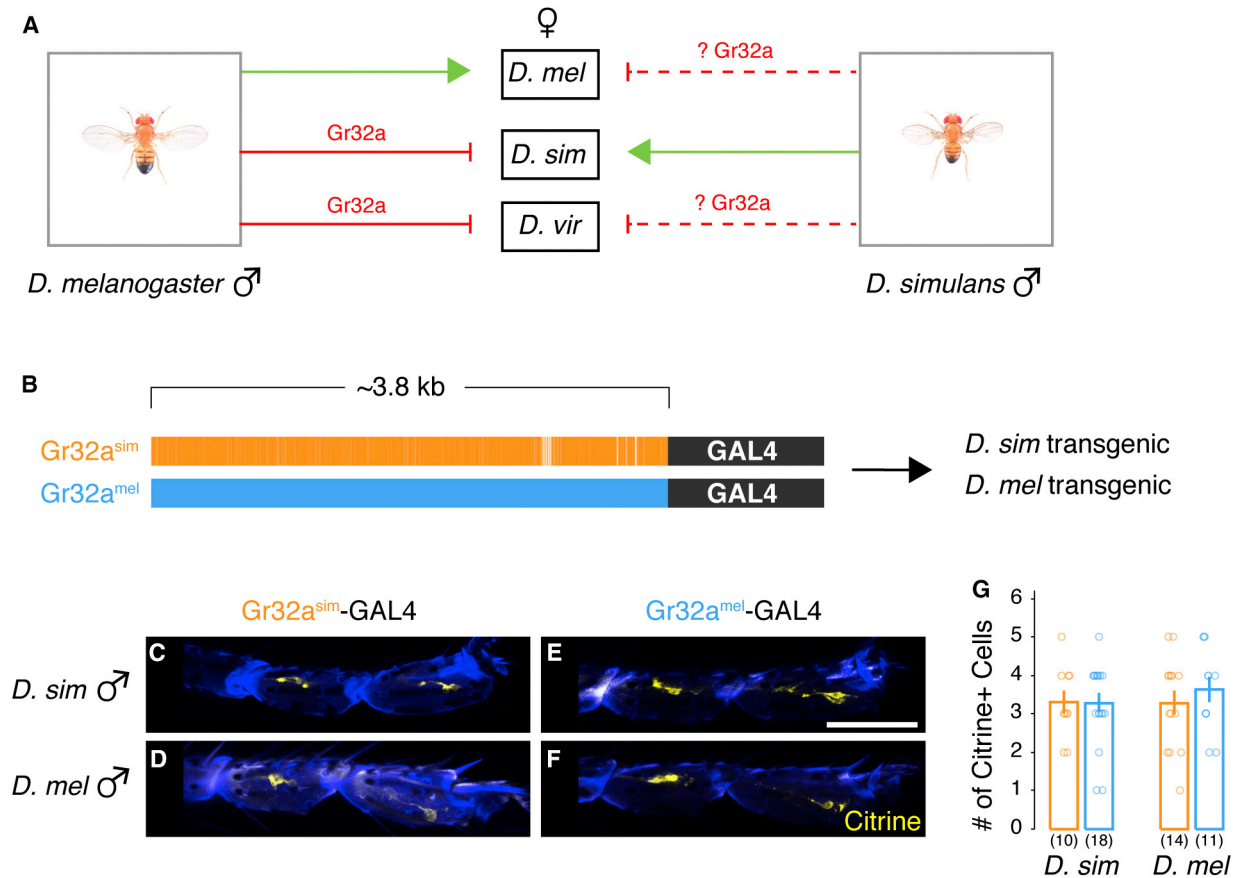
Figure 2. A Regulatory Region in the *Gr32a* Locus Is Functionally Conserved

(A) We sought to determine whether, similar to *D. melanogaster*, Gr32a was expressed in *D. simulans* foreleg tarsi.

(B) Schematic of transgenic constructs using a DNA sequence 5′ of Gr32a start codon from *D. simulans* (orange) and *D. melanogaster* (blue) to drive GAL4 expression. Sequence identity in this region between the two species is noted by solid orange color.

(C–F) Gr32a^{sim}-GAL4 (C and D) and Gr32a^{mel}-GAL4 (E and F) each drive comparable citrine expression in distal tarsal segments T4 and T5 in both *D. simulans* (C and E) and *D. melanogaster* (D and F) male forelegs.

(G) Quantification of data shown in histological panels (C–F).

Mean ± SEM. Each circle denotes the number of citrine+ cells per male foreleg tarsi per genotype. n = 11–18 per genotype. Scale bar, 50 μm. See also Table S1 and Figure S1.

chemosensory organs known to express Gr32a (Scott et al., 2001; Wang et al., 2004). Similar stretches of genomic DNA are also sufficient to drive reporter expression of other Grs (Weiss et al., 2011), indicating a conserved regulatory logic of expression for this gene family in *D. melanogaster*. We subcloned ~3.8 kb of genomic DNA upstream of the *D. simulans* Gr32a start codon and used it to drive GAL4 expression (Gr32a^{sim}-GAL4) in transgenic *D. simulans* and *D. melanogaster* flies (Figure 2B). Transgene expression was visualized via the fluorescent reporter citrine (Inagaki et al., 2014) (Figures 2C and 2D). We observed citrine expression in three or four neurons in T4–T5 tarsal segments of *D. simulans* and *D. melanogaster*, demonstrating that regulatory sequences in the *D. simulans* Gr32a locus drive reporter expression in foreleg tarsi of both species (Figures 2C, 2D, and 2G). Moreover, the projections of Gr32a sensory neurons in the subesophageal zone (SEZ) appeared similar between

the two species (Figures S1K and S1L), indicative of a shared peripheral expression pattern (Wang et al., 2004).

We next tested whether the ~3.8 kb regulatory DNA sequence from these two species drives expression in the same tarsal neurons. We generated *D. melanogaster* flies harboring GAL4 under control of conspecific ~3.8 kb DNA sequence 5′ of Gr32a such that this transgene (Gr32a^{mel}-GAL4) was inserted into the same landing site that we had used for Gr32a^{sim}-GAL4 (Figures 2B, 2D, and 2F). Importantly, Gr32a^{mel}-GAL4 regulated reporter expression in *D. melanogaster* foreleg tarsi, as described previously for other GAL4 alleles of Gr32a (Fan et al., 2013; Miyamoto and Amrein, 2008; Moon et al., 2009; Scott et al., 2001). In *D. melanogaster* flies bearing both Gr32a^{mel}-GAL4 and Gr32a^{sim}-GAL4, we observed a similar number of citrine+ foreleg tarsal neurons compared with flies bearing these GAL4 drivers individually (Figure S1C). Together, these data are consistent with the notion that the upstream regulatory region of Gr32a in
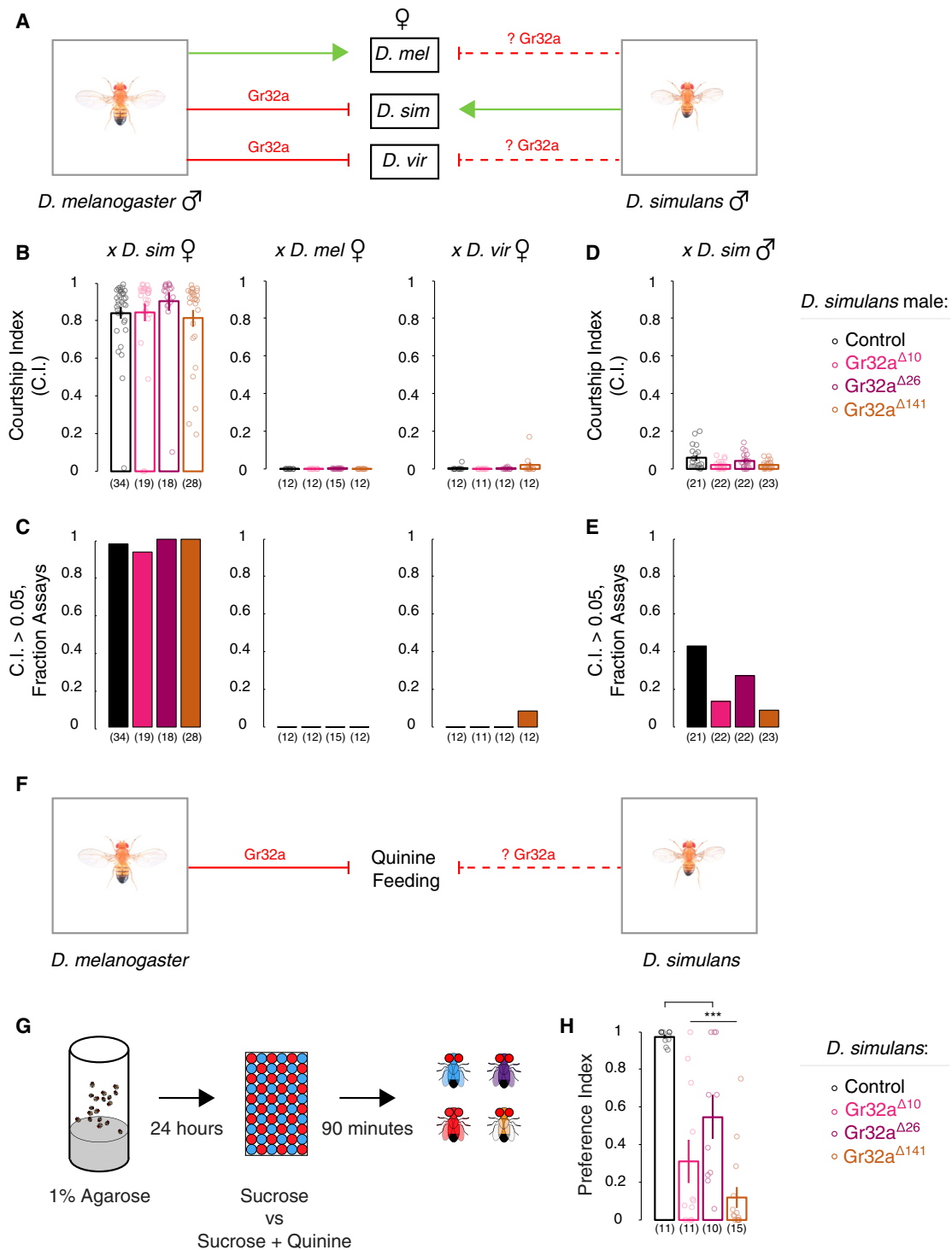
A

♀

D. mel   ? Gr32a

Gr32a   D. sim

Gr32a   D. vir   ? Gr32a

D. melanogaster ♂   *D. simulans* ♂

B   x *D. sim* ♀   x *D. mel* ♀   x *D. vir* ♀   **D**   x *D. sim* ♂

Courtship Index (C.I.)

(34) (19) (18) (28)   (12) (12) (15) (12)   (12) (11) (12) (12)   (21) (22) (22) (23)

D. simulans male:
○ Control
○ Gr32a$^{\Delta 10}$
○ Gr32a$^{\Delta 26}$
○ Gr32a$^{\Delta 141}$

C   C.I. > 0.05, Fraction Assays

(34) (19) (18) (28)   (12) (12) (15) (12)   (12) (11) (12) (12)

E   C.I. > 0.05, Fraction Assays

(21) (22) (22) (23)

F

D. melanogaster   Gr32a   Quinine Feeding   ? Gr32a   *D. simulans*

G

1% Agarose   24 hours   Sucrose vs Sucrose + Quinine   90 minutes

H

Preference Index

***

(11) (11) (10) (15)

D. simulans:
○ Control
○ Gr32a$^{\Delta 10}$
○ Gr32a$^{\Delta 26}$
○ Gr32a$^{\Delta 141}$

Figure 3. Gr32a Is Not Required to Inhibit Interspecies Courtship but Is Essential for Quinine Sensing in *D. simulans*
(A) We tested whether, similar to *D. melanogaster* males, Gr32a inhibits interspecies courtship by *D. simulans* males.
(B and C) WT and Gr32a mutant *D. simulans* males court conspecific but not *D. melanogaster* or *D. virilis* females.
(D and E) WT and Gr32a mutant *D. simulans* males show similar low levels of courtship toward conspecific males.
(F) We tested whether, similar to *D. melanogaster*, Gr32a inhibits feeding on quinine-containing food in *D. simulans*.
(G) Schematic of feeding assay for starved *D. simulans* given choice of colored food containing sucrose or sucrose and quinine. Flies with blue, red, purple, or no food dye colored abdomens were enumerated after exposure to food for 90 min.

(legend continued on next page)

the two species is functionally conserved and sufficient to drive expression in the same foreleg tarsi neurons of *D. melanogaster*.

We next tested whether the ~3.8 kb genomic DNA 5′ of *D. melanogaster* Gr32a start codon would drive expression in foreleg tarsal neurons of *D. simulans*. We inserted Gr32a^mel^-GAL4 into the landing site we used to generate *D. simulans* flies bearing Gr32a^sim^-GAL4 (Figures 2B and 2E). We observed reporter expression in three or four neurons restricted to T4–T5 tarsal segments of *D. simulans* in a pattern mirroring that observed in *D. simulans* bearing Gr32a^sim^-GAL4 (Figures 2C, 2E, and 2G). Given that all GAL4 and UAS transgenes we built in *D. simulans* were inserted into a single landing site that afforded us reliable and non-leaky expression, we could not directly test whether the same neurons were labeled by Gr32a^sim^-GAL4 and Gr32a^mel^-GAL4 in this species. Nevertheless, our findings strongly suggest that similar *cis* and *trans* regulatory features regulate Gr32a expression in foreleg tarsi of the two species.

We find that the ~3.8 kb of regulatory genomic DNA is conserved in multiple insects (mean nucleotide conservation phyloP score = 1.4; see Figures S1D–S1F). Coding exons for another gene (*D. melanogaster CG6201*) contribute to this sequence similarity, but some of the most conserved blocks of sequence are intergenic regions (Figure S1E). Overall, nucleotide substitutions have occurred in this region at 42.5% the rate of 4-fold degenerate sites in protein-coding exons, slower than expected under a neutral model of DNA evolution ($p < 1 \times 10^{-5}$; see STAR Methods for details; Figure S1F). Within *D. melanogaster* and *D. simulans*, >95% of the DNA sequence is identical across this ~3.8 kb region. To examine sequence differences at single-nucleotide resolution, we tested each position for a faster or slower rate of DNA substitutions in *D. melanogaster* than expected, given the rate in *D. simulans* and 25 other insects. We also conducted the comparable test for *D. simulans*. This analysis revealed that few bases in the ~3.8 kb region are evolving faster than expected (>99% bases with phyloP score > -2; Figures S1G and S1H). Because the ~3.8 kb region is highly conserved and *D. melanogaster* and *D. simulans* diverged from a common ancestor only recently, it was difficult to detect whether this stretch of DNA is evolving slower than expected subsequent to speciation from this shared ancestor. Together, our findings show that this ~3.8 kb region is conserved in sequence and function in *D. melanogaster* and *D. simulans* such that it is sufficient to drive expression in neurons of foreleg tarsi.

Gr32a and Gr33a Are Not Essential to Inhibit Interspecies Courtship in *D. simulans* Males

We tested whether Gr32a was essential to inhibit interspecies courtship in *D. simulans* males (Figure 3A). We targeted distinct sequences in the first coding exon of *D. simulans* Gr32a to generate three different mutant alleles via the CRISPR/Cas9 system (Figures S2A–S2C). Two of the alleles (Gr32a^Δ10^ and Gr32a^Δ26^) are predicted to lead to 10 and 26 bp deletions in the first coding exon that result in a frameshift and premature stop codon; these likely encode a non-functional Gr32a chemoreceptor protein (Figures S2C and S2D). The third allele (Gr32a^Δ141^) has a 141 bp deletion that is predicted to eliminate 47 amino acids from the predicted N-terminal intracellular domain of this chemoreceptor (Figures S2B–S2D, S2F, and S2G). We next tested *D. simulans* males homozygous mutant for these Gr32a alleles for courtship displays toward conspecifics and members of other species. We observed that each of the three mutants courted conspecific females similar to WT controls (Figures 3B and 3C). Moreover, these mutants did not increase courtship toward conspecific males or *D. melanogaster*, *D. yakuba*, or *D. virilis* females (Figures 3B–3E and S2E). Our findings indicate a divergence in behavioral function of Gr32a between *D. simulans* and *D. melanogaster*, a conclusion consistent with previous sequence analyses showing that bitter-sensing Grs such as Gr32a may be evolving rapidly (Gardiner et al., 2009; McBride et al., 2007). In summary, Gr32a mutant *D. simulans* males do not show elevated courtship toward other species, a finding in sharp contrast to Gr32a-null *D. melanogaster* males, which court other species avidly (Fan et al., 2013).

Gr33a is co-expressed with Gr32a in foreleg tarsi in *D. melanogaster*, and it is required to inhibit intermale but not interspecies courtship in males of this species (Fan et al., 2013; Moon et al., 2009). Gr33a is also encoded in the *D. simulans* genome (Drosophila 12 Genomes Consortium et al., 2007), and we wondered if this chemoreceptor had evolved to inhibit interspecies courtship in this species. Using CRISPR/Cas9, we generated two mutant alleles of Gr33a, one with a 10 bp deletion (Gr33a^Δ10^) that leads to a frameshift and premature stop codon and the other encompassing an in-frame deletion (96 bp, Gr33a^Δ96^) (Figures S3A–S3D). Male *D. simulans* mutant for each of these alleles courted conspecific females similar to WT controls and did not increase courtship toward conspecific males or *D. melanogaster*, *D. yakuba*, or *D. virilis* females (Figures S3E–S3H). Together, our results indicate that chemosensory receptor-mediated inhibition of courtship toward reproductively futile targets (conspecific males and members of other species) has diverged between the closely related *D. melanogaster* and *D. simulans*.

Both Gr32a and Gr33a Are Required in *D. simulans* to Detect Quinine

In *D. melanogaster*, Gr32a and Gr33a are also essential for a behavioral aversion to quinine, a bitter tastant (Lee et al., 2010; Moon et al., 2009). Chemoreceptors can evolve to facilitate food sensing in different ecological niches (Baldwin et al., 2014; Jordt and Julius, 2002; Prieto-Godino et al., 2017; Wisotsky et al., 2011). Given the divergence of behavioral function of

---

(H) Significant decrease in preference by *Gr32a* mutant *D. simulans* for food containing only sucrose.

Mean ± SEM. In (B)–(E), each circle denotes CI of one male, and n = 11–34 per genotype. In (G) and (H), preference index = {(# flies that ate sucrose-only food + 0.5*(purple flies)}/(number of flies that ate). Each circle denotes the preference index for one experiment. For each experiment, 106 ± 6 *D. simulans* of each genotype were used. n = 11–15 experiments/genotype. ***p < 0.001. See Tables S1–S3 and Figures S2 and S3.

Gr32a between *D. melanogaster* and *D. simulans*, we wondered if Gr32a and Gr33a were required in *D. simulans* for a response to quinine (Figures 3F and S3I). We tested this in a feeding preference assay in which starved flies were offered a choice between food containing a low concentration of sugar (1 mM sucrose) or a high concentration of sugar (5 mM sucrose) spiked with quinine (0.5 mM) (Montell, 2009; Moon et al., 2009; Tanimura et al., 1982) (Figure 3G). WT *D. simulans* preferred feeding on the low concentration of sugar, whereas flies mutant for either Gr32a or Gr33a showed reduced preference for feeding on sugar alone (Figures 3H and S3J). Although all mutant lines showed a loss of preference for feeding on sugar alone, there was some variability in the phenotypes observed for the different alleles. Such variability likely resulted from subtle differences in the assay conditions or genetic background; consistent with this notion, there was no statistical difference in behavior between flies bearing the largest and smallest deletions for both genes. It is possible that all *D. simulans* Gr32a and Gr33a mutations we have generated disrupt sensing quinine but not chemosensory cues from other species, a notion that could be tested when deficiencies spanning Gr32a and Gr33a become available in this species. Our present findings show that quinine sensing via Gr32a and Gr33a is conserved between *D. melanogaster* and *D. simulans*.

Ppk25 Promotes Conspecific Courtship in *D. simulans* Males

Our findings show that chemosensory receptor mechanisms that inhibit courtship of reproductively futile targets in *D. melanogaster* are not used in *D. simulans*. We wondered whether genetic loci that promote courtship had also differentiated between these two species. Many loci promote courtship of *D. melanogaster* males toward conspecific females (reviewed in Dickson, 2008; Yamamoto and Koganezawa, 2013). We chose to test the function of the Ppk25 pickpocket ion channel subunit that is expressed in foreleg tarsi chemosensory neurons and appears to exclusively promote courtship in *D. melanogaster* (Figure 4A) (Clowney et al., 2015; Kallman et al., 2015; Lin et al., 2005; Starostina et al., 2012; Vijayan et al., 2014). We generated two alleles of Ppk25 in *D. simulans* via CRISPR/Cas9, a 2 bp insertion and a 4 bp deletion in the first coding exon, that are predicted to lead to frameshifts and premature stop codons and are likely to be null mutations (Figures S4A–S4D). *D. melanogaster* Ppk25 is required for male courtship in the dark (Boll and Noll, 2002; Jezovit et al., 2017; Kohatsu and Yamamoto, 2015; Krstic et al., 2009; Lin et al., 2005; Spieth, 1974). Unlike *D. melanogaster*, *D. simulans* males court conspecific females vigorously only under bright illumination (Grossfield, 1971; Jezovit et al., 2017) (Figures S4E and S4F). Furthermore, this requirement for bright illumination in *D. simulans* overrides courtship disinhibition following tarsectomy (Figure S4G). We tested whether Ppk25 modulated courtship by *D. simulans* males in bright light or dark conditions. *D. simulans* males mutant for Ppk25 showed reduced courtship of conspecific females in the dark (Figures 4B and 4C). These mutants also showed subtle, but significant, reduction in courtship under bright illumination, suggesting a more stringent requirement for Ppk25 in courtship in this species (Figures 4D and 4E). *D. simulans* males mutant for

Ppk25 did not display elevated courtship to other drosophilids (Figures S4H and S4I), indicating that it does not function in this species to inhibit interspecies courtship. In fact, we found that compared with WT males, Ppk25 mutant *D. simulans* showed reduced courtship of *D. yakuba* females (Figures S4H and S4I). In summary, Ppk25 functions in both *D. melanogaster* and *D. simulans* to promote WT courtship displays.

DISCUSSION

Changes in morphological or other traits across evolution continue to be vigorously investigated (Carroll, 2008). We have examined whether the Gr32a+ chemosensory pathway that inhibits interspecies courtship in *D. melanogaster* functions similarly in *D. simulans*. We find that although *D. simulans* Gr32a is expressed in foreleg tarsi, similar to its counterpart in *D. melanogaster*, it is not required to inhibit interspecies courtship. It is possible that Gr32a neurons in foreleg tarsi still function to inhibit this behavior, a notion we attempted to address experimentally by inactivating Gr32a+ neurons. However, it was technically challenging to generate the requisite reagents required (Kir2.1, tetanus toxin light chain, *shibire^ts*) (Luo et al., 2008) in this species, despite numerous attempts. *D. simulans* males sense aversive cues on the cuticle of *D. melanogaster* females (Billeter et al., 2009; Coyne et al., 1994; Ferveur, 2005; Jallon, 1984). Given that Gr32a is not essential for this function, what chemoreceptors might be used to detect such repellents in *D. simulans*? It is possible that in this species, *Gr32a* and *Gr33a* function redundantly to inhibit interspecies courtship, a hypothesis difficult to test directly because these loci are only 1 Mb apart in the genome. Regardless, our findings still demonstrate a divergence in the function of Gr32a between *D. melanogaster* and *D. simulans*. The gustatory and ionotropic chemoreceptor families contain many members, and our results are also consistent with the idea that a different chemoreceptor(s) functions to inhibit interspecies courtship by *D. simulans* males (Joseph and Carlson, 2015). Although changes in centrally located courtship circuits may confer species-specific pheromonal responses (Seeholzer et al., 2018), our results show that there is divergence in chemoreceptor-mediated suppression of interspecific courtship between *D. melanogaster* and *D. simulans* (Figure 4F). In other words, our findings show that these closely related species use distinct peripheral chemosensory pathways to suppress interspecific courtship.

The divergence in chemoreceptor-mediated suppression of courtship between *D. melanogaster* and *D. simulans* does not reflect a global reorganization of molecular pathways that regulate courtship (Figure 4F). We find that similar to its role in *D. melanogaster*, Ppk25 is required to promote courtship toward conspecific females in *D. simulans*. Ppk25 is required to sense 7,11-heptacosadiene, an aphrodisiac cue, in *D. melanogaster* (Kallman et al., 2015; Starostina et al., 2012); however, 7,11-heptacosadiene is an aversive cue for *D. simulans* males (Billeter et al., 2009), so it will be interesting to understand how Ppk25 functions in both species to promote conspecific courtship. Although 7,11-heptacosadiene serves as a cuticular attractant to *D. melanogaster* males, elimination of all cuticular pheromones in *D. melanogaster* females does not eliminate courtship
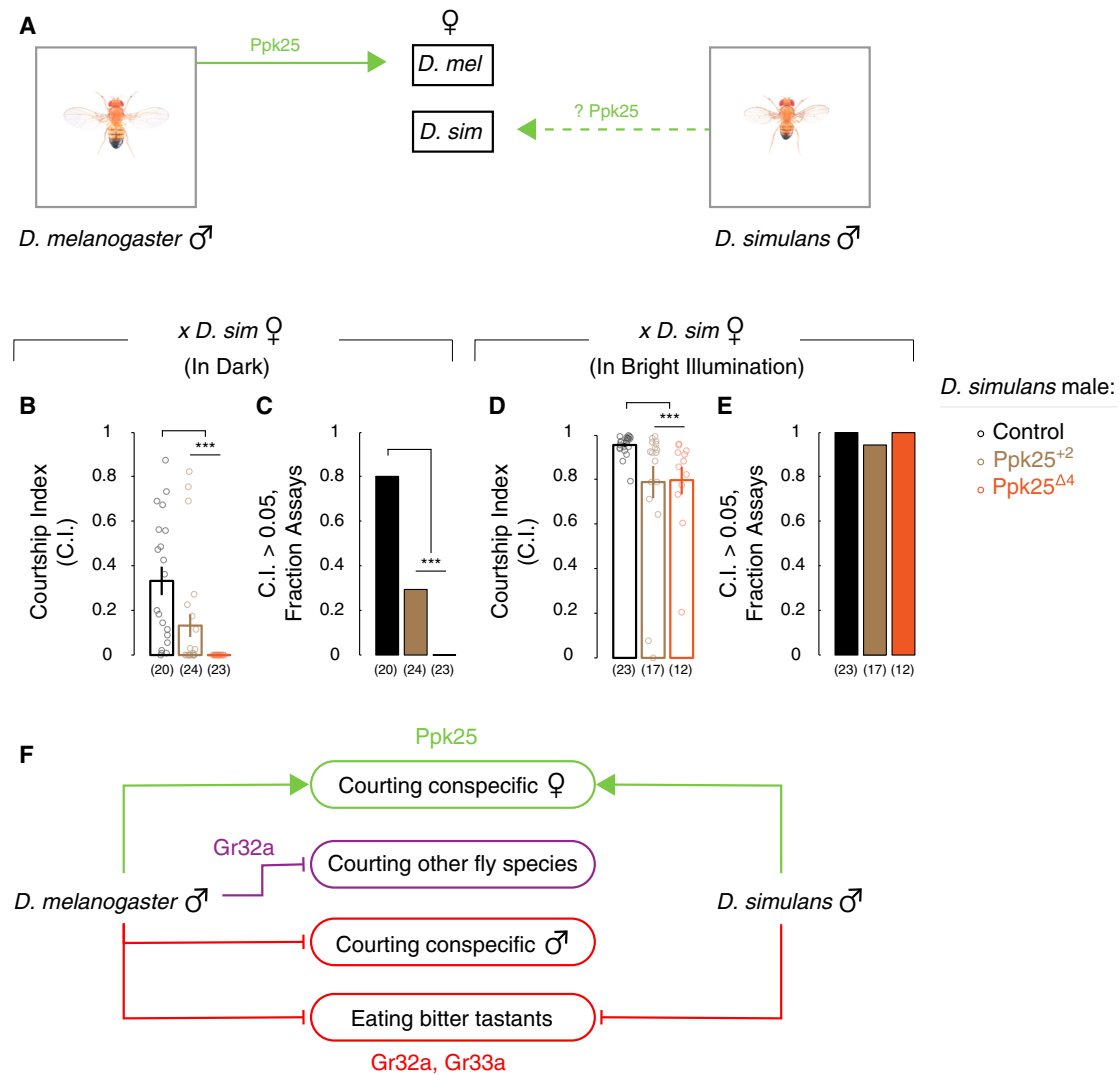
Figure 4. Ppk25 Promotes Conspecific Courtship by *D. simulans* Males

(A) We tested whether, similar to *D. melanogaster*, Ppk25 promotes conspecific courtship by *D. simulans* males.

(B–D) *Ppk25* mutant *D. simulans* males show decreased courtship index (C.I.) in dark (B) and bright illumination (D) and a reduction in high levels of C.I. in dark (C) but not bright illumination (E) toward conspecific females.

(E) No difference between WT and *Ppk25* mutant *D. simulans* males in percentage assays with high levels of courtship of conspecific females.

(F) Summary of the roles of Gr32a, Gr33a, and Ppk25 in *D. melanogaster* and *D. simulans*.

Mean ± SEM. Each circle denotes CI for one male. n = 12–24 per genotype. ***p < 0.001. See Tables S1 and S3 and Figure S4.

by *D. melanogaster* males, and in fact, it disinhibits courtship by *D. simulans* males (Billeter et al., 2009; Coyne et al., 1994; Savarit et al., 1999). Thus cuticular attractants are not essential for courtship and anti-aphrodisiacs may guide avoidance of courtship with reproductively futile targets such as individuals of other species; together with our previous findings (Fan et al., 2013), our results show that Gr32a is essential for detection of such aversive compounds by *D. melanogaster* but not *D. simulans* males.

Both Gr32a and Gr33a are required for avoidance of quinine in *D. melanogaster* and *D. simulans*. Thus, the chemosensory functions of Gr32a and Gr33a in avoiding quinine and inhibiting courtship of reproductively futile targets are evolutionarily dissociable

(Figure 4F). The same behavioral trait (tapping) and sensorimotor appendage (foreleg) inhibit courting of reproductively dead-end targets in *D. melanogaster* and *D. simulans*, but our studies show that the molecular mechanisms that preclude such courtship have diverged between these species. Previous work from our and other labs shows that different genetic pathways control distinct quantitative aspects of behavioral subroutines (Ding et al., 2016; Greenwood et al., 2013; Weber et al., 2013; Xu et al., 2012). Together, these findings demonstrate that modifications in genetic pathways can be used to gate a behavior or to implement quantitative changes in that behavior. We also find that although chemoreceptor mechanisms inhibiting

interspecies courtship have differentiated between closely related species, a chemosensory pathway promoting courtship appears to have a similar positive valence in both species. It will be interesting to determine whether these courtship-promoting and courtship-inhibiting pathways evolve in a similar pattern across other drosophilid species. Alternatively (Jacob, 1977; Luo, 2015), our findings may reflect the idiosyncratic nature of selective forces that exploit mutations in apparently random pathways to effect evolutionary change. It should be possible to distinguish between these alternatives by studying mechanisms that regulate courtship in additional drosophilid species.

STAR★METHODS

Detailed methods are provided in the online version of this paper and include the following:

- KEY RESOURCES TABLE
- CONTACT FOR REAGENT AND RESOURCE SHARING
- EXPERIMENTAL MODEL AND SUBJECT DETAILS
- METHOD DETAILS
  - Generating D. simulans Gr32a, Gr33a, or Ppk25 mutants
  - Generating D. simulans and *D. melanogaster* transgenic animals
  - Molecular analysis of Gr32a, Gr33a, and Ppk25 mutations in D. simulans
  - Histology
  - Courtship assays
  - Taste assay
  - Tests for Non-Neutral Evolution
  - Hydrophobicity plot
- QUANTIFICATION AND STATISTICAL ANALYSIS

AUTHOR CONTRIBUTIONS

O.M.A. and N.M.S. designed the fly experiments. O.M.A., K.M.T., P.H.S., and J.P. conducted the fly experiments and analyzed behavioral data. A.A.-H. and K.S.P. conducted bioinformatics analyses of Gr32a ∼3.8 kb regulatory region. S.P. helped with molecular analysis of Gr33a and Ppk25 mutants. G.W.D. provided invaluable advice, resources, and laboratory space for some of these experiments. J.-M.K. and D.L.S. provided reagents to generate transgenic *D. simulans* lines. O.M.A., A.A.-H., K.S.P., and N.M.S. wrote the paper.

REFERENCES

Allaire, J.J., Cheng, J., Xie, Y., McPherson, J., Chang, W., Allen, J., Wickham, H., Atkins, A., Hyndman, R., and Arslan, R. (2017). rmarkdown: Dynamic Documents for R. https://cran.r-project.org/web/packages/rmarkdown/index.html.

Artimo, P., Jonnalagedda, M., Arnold, K., Baratin, D., Csardi, G., de Castro, E., Duvaud, S., Flegel, V., Fortier, A., Gasteiger, E., et al. (2012). ExPASy: SIB bioinformatics resource portal. Nucleic Acids Res. *40*, W597–W603.

Baldwin, M.W., Toda, Y., Nakagita, T., O'Connell, M.J., Klasing, K.C., Misaka, T., Edwards, S.V., and Liberles, S.D. (2014). Sensory biology. Evolution of sweet taste perception in hummingbirds by transformation of the ancestral umami receptor. Science *345*, 929–933.

Bastock, M., and Manning, A. (1955). The courtship of Drosophila melanogaster. Behaviour *8*, 85–111.

Billeter, J.-C., Atallah, J., Krupp, J.J., Millar, J.G., and Levine, J.D. (2009). Specialized cells tag sexual and species identity in Drosophila melanogaster. Nature *461*, 987–991.

Blanchette, M., Kent, W.J., Riemer, C., Elnitski, L., Smit, A.F., Roskin, K.M., Baertsch, R., Rosenbloom, K., Clawson, H., Green, E.D., et al. (2004). Aligning multiple genomic sequences with the threaded blockset aligner. Genome Res. *14*, 708–715.

Boll, W., and Noll, M. (2002). The Drosophila Pox neuro gene: control of male courtship behavior and fertility as revealed by a complete dissection of all enhancers. Development *129*, 5667–5681.

Carroll, S.B. (2008). Evo-devo and an expanding evolutionary synthesis: a genetic theory of morphological evolution. Cell *134*, 25–36.

Clowney, E.J., Iguchi, S., Bussell, J.J., Scheer, E., and Ruta, V. (2015). Multimodal chemosensory circuits controlling male courtship in Drosophila. Neuron *87*, 1036–1049.

Coyne, J.A., and Orr, H.A. (1989). Patterns of speciation in Drosophila. Evolution *43*, 362–381.

Coyne, J.A., Crittenden, A.P., and Mah, K. (1994). Genetics of a pheromonal difference contributing to reproductive isolation in Drosophila. Science *265*, 1461–1464.

Darwin, C. (1860). On the Origin of Species by Means of Natural Selection, or, the Preservation of Favoured Races in the Struggle for Life (Appleton).

David, J.R., Lemeunier, F., Tsacas, L., and Yassin, A. (2007). The historical discovery of the nine species in the Drosophila melanogaster species subgroup. Genetics *177*, 1969–1973.

Demir, E., and Dickson, B.J. (2005). Fruitless splicing specifies male courtship behavior in Drosophila. Cell *121*, 785–794.

Dickson, B.J. (2008). Wired for sex: the neurobiology of Drosophila mating decisions. Science *322*, 904–909.

Ding, Y., Berrocal, A., Morita, T., Longden, K.D., and Stern, D.L. (2016). Natural courtship song variation caused by an intronic retroelement in an ion channel gene. Nature *536*, 329–332.

Dobzhansky, T. (1937). Genetic nature of species differences. Am. Nat. 71, 404–420.

Drosophila 12 Genomes Consortium; Clark, A.G., Eisen, M.B., Smith, D.R., Bergman, C.M., Oliver, B., Markow, T.A., Kaufman, T.C., Kellis, M., Gelbart, W., et al. (2007). Evolution of genes and genomes on the Drosophila phylogeny. Nature 450, 203–218.

Everaerts, C., Farine, J.-P., Cobb, M., and Ferveur, J.-F. (2010). Drosophila cuticular hydrocarbons revisited: mating status alters cuticular profiles. PLoS ONE 5, e9607.

Fan, P., Manoli, D.S., Ahmed, O.M., Chen, Y., Agarwal, N., Kwong, S., Cai, A.G., Neitz, J., Renslo, A., Baker, B.S., and Shah, N.M. (2013). Genetic and neural mechanisms that inhibit Drosophila from mating with other species. Cell 154, 89–102.

Ferveur, J.-F. (2005). Cuticular hydrocarbons: their evolution and roles in Drosophila pheromonal communication. Behav. Genet. 35, 279–295.

Gardiner, A., Butlin, R.K., Jordan, W.C., and Ritchie, M.G. (2009). Sites of evolutionary divergence differ between olfactory and gustatory receptors of Drosophila. Biol. Lett. 5, 244–247.

Gill, K.S. (1963). A mutation causing abnormal courtship and mating behavior in males of Drosophila melanogaster. Am. Zool. 3, 507.

Gokcezade, J., Sienski, G., and Duchek, P. (2014). Efficient CRISPR/Cas9 plasmids for rapid and versatile genome editing in Drosophila. G3 (Bethesda) 4, 2279–2282.

Greenspan, R.J., and Ferveur, J.F. (2000). Courtship in Drosophila. Annu. Rev. Genet. 34, 205–232.

Greenwood, A.K., Wark, A.R., Yoshida, K., and Peichel, C.L. (2013). Genetic and neural modularity underlie the evolution of schooling behavior in threespine sticklebacks. Curr. Biol. 23, 1884–1888.

Grossfield, J. (1971). Geographic distribution and light-dependent behavior in Drosophila. Proc. Natl. Acad. Sci. U S A 68, 2669–2673.

Groth, A.C., Fish, M., Nusse, R., and Calos, M.P. (2004). Construction of transgenic Drosophila by using the site-specific integrase from phage phiC31. Genetics 166, 1775–1782.

Hall, J.C. (1978). Courtship among males due to a male-sterile mutation in Drosophila melanogaster. Behav. Genet. 8, 125–141.

Hall, J.C. (1994). The mating of a fly. Science 264, 1702–1714.

Hotta, Y., and Benzer, S. (1976). Courtship in Drosophila mosaics: sex-specific foci for sequential action patterns. Proc. Natl. Acad. Sci. U S A 73, 4154–4158.

Inagaki, H.K., Jung, Y., Hoopfer, E.D., Wong, A.M., Mishra, N., Lin, J.Y., Tsien, R.Y., and Anderson, D.J. (2014). Optogenetic control of Drosophila using a red-shifted channelrhodopsin reveals experience-dependent influences on courtship. Nat. Methods 11, 325–332.

Jacob, F. (1977). Evolution and tinkering. Science 196, 1161–1166.

Jallon, J.M. (1984). A few chemical words exchanged by Drosophila during courtship and mating. Behav. Genet. 14, 441–478.

Jezovit, J.A., Levine, J.D., and Schneider, J. (2017). Phylogeny, environment and sexual communication across the Drosophila genus. J. Exp. Biol. 220, 42–52.

Jordt, S.-E., and Julius, D. (2002). Molecular basis for species-specific sensitivity to "hot" chili peppers. Cell 108, 421–430.

Joseph, R.M., and Carlson, J.R. (2015). Drosophila chemoreceptors: a molecular interface between the chemical world and the brain. Trends Genet. 31, 683–695.

Kallman, B.R., Kim, H., and Scott, K. (2015). Excitation and inhibition onto central courtship neurons biases Drosophila mate choice. eLife 4, e11188.

Karolchik, D., Hinrichs, A.S., Furey, T.S., Roskin, K.M., Sugnet, C.W., Haussler, D., and Kent, W.J. (2004). The UCSC Table Browser data retrieval tool. Nucleic Acids Res. 32, D493–D496.

Knapp, J.-M., Chung, P., and Simpson, J.H. (2015). Generating customized transgene landing sites and multi-transgene arrays in Drosophila using phiC31 integrase. Genetics 199, 919–934.

Koganezawa, M., Haba, D., Matsuo, T., and Yamamoto, D. (2010). The shaping of male courtship posture by lateralized gustatory inputs to male-specific interneurons. Curr. Biol. 20, 1–8.

Kohatsu, S., and Yamamoto, D. (2015). Visually induced initiation of Drosophila innate courtship-like following pursuit is mediated by central excitatory state. Nat. Commun. 6, 6457.

Kohatsu, S., Koganezawa, M., and Yamamoto, D. (2011). Female contact activates male-specific interneurons that trigger stereotypic courtship behavior in Drosophila. Neuron 69, 498–508.

Krstic, D., Boll, W., and Noll, M. (2009). Sensory integration regulating male courtship behavior in Drosophila. PLoS ONE 4, e4457.

Lacaille, F., Hiroi, M., Twele, R., Inoshita, T., Umemoto, D., Manière, G., Marion-Poll, F., Ozaki, M., Francke, W., Cobb, M., et al. (2007). An inhibitory sex pheromone tastes bitter for Drosophila males. PLoS ONE 2, e661.

Lee, Y., Kim, S.H., and Montell, C. (2010). Avoiding DEET through insect gustatory receptors. Neuron 67, 555–561.

Lin, H., Mann, K.J., Starostina, E., Kinser, R.D., and Pikielny, C.W. (2005). A Drosophila DEG/ENaC channel subunit is required for male response to female pheromones. Proc. Natl. Acad. Sci. U S A 102, 12831–12836.

Lin, H.-H., Cao, D.-S., Sethi, S., Zeng, Z., Chin, J.S.R., Chakraborty, T.S., Shepherd, A.K., Nguyen, C.A., Yew, J.Y., Su, C.-Y., and Wang, J.W. (2016). Hormonal modulation of pheromone detection enhances male courtship success. Neuron 90, 1272–1285.

Luo, L. (2015). Principles of Neurobiology (Garland Science).

Luo, L., Callaway, E.M., and Svoboda, K. (2008). Genetic dissection of neural circuits. Neuron 57, 634–660.

Manning, A. (1959). The sexual isolation between Drosophila melanogaster and Drosophila simulans. Anim. Behav. 7, 60–65.

Manoli, D.S., Foss, M., Villella, A., Taylor, B.J., Hall, J.C., and Baker, B.S. (2005). Male-specific fruitless specifies the neural substrates of Drosophila courtship behaviour. Nature 436, 395–400.

Markow, T.A. (2015). The secret lives of Drosophila flies. eLife 4.

Mayr, E. (1988). The why and how of species. Biol. Philos. 3, 431–441.

Mayr, E., and Dobzhansky, T. (1945). Experiments on sexual isolation in Drosophila: IV. Modification of the degree of isolation between Drosophila pseudoobscura and Drosophila persimilis and sexual preferences in Drosophila prosoltans. Proc. Natl. Acad. Sci. U S A 31, 75–82.

McBride, C.S., Arguello, J.R., and O'Meara, B.C. (2007). Five Drosophila genomes reveal nonneutral evolution and the signature of host specialization in the chemoreceptor superfamily. Genetics 177, 1395–1416.

Mendelson, T.C. (2003). Sexual isolation evolves faster than hybrid inviability in a diverse and sexually dimorphic genus of fish (Percidae: Etheostoma). Evolution 57, 317–327.

Miyamoto, T., and Amrein, H. (2008). Suppression of male courtship by a Drosophila pheromone receptor. Nat. Neurosci. 11, 874–876.

Montell, C. (2009). A taste of the Drosophila gustatory receptors. Curr. Opin. Neurobiol. 19, 345–353.

Moon, S.J., Lee, Y., Jiao, Y., and Montell, C. (2009). A Drosophila gustatory receptor essential for aversive taste and inhibiting male-to-male courtship. Curr. Biol. 19, 1623–1627.

Neph, S., Kuehn, M.S., Reynolds, A.P., Haugen, E., Thurman, R.E., Johnson, A.K., Rynes, E., Maurano, M.T., Vierstra, J., Thomas, S., et al. (2012). BEDOPS: high-performance genomic feature operations. Bioinformatics 28, 1919–1920.

Orr, H.A. (2005). The genetic basis of reproductive isolation: insights from Drosophila. Proc. Natl. Acad. Sci. U S A 102 (Suppl 1), 6522–6526.

Orr, H.A., Masly, J.P., and Presgraves, D.C. (2004). Speciation genes. Curr. Opin. Genet. Dev. 14, 675–679.

Pavlou, H.J., and Goodwin, S.F. (2013). Courtship behavior in Drosophila melanogaster: towards a 'courtship connectome'. Curr. Opin. Neurobiol. 23, 76–83.

Pfeiffer, B.D., Jenett, A., Hammonds, A.S., Ngo, T.T., Misra, S., Murphy, C., Scully, A., Carlson, J.W., Wan, K.H., Laverty, T.R., et al. (2008). Tools for

neuroanatomy and neurogenetics in Drosophila. Proc. Natl. Acad. Sci. USA *105*, 9715–9720.

Pfeiffer, B.D., Ngo, T.-T.B., Hibbard, K.L., Murphy, C., Jenett, A., Truman, J.W., and Rubin, G.M. (2010). Refinement of tools for targeted gene expression in Drosophila. Genetics *186*, 735–755.

Pollard, K.S., Hubisz, M.J., Rosenbloom, K.R., and Siepel, A. (2010). Detection of nonneutral substitution rates on mammalian phylogenies. Genome Res. *20*, 110–121.

Prieto-Godino, L.L., Rytz, R., Cruchet, S., Bargeton, B., Abuin, L., Silbering, A.F., Ruta, V., Dal Peraro, M., and Benton, R. (2017). Evolution of acid-sensing olfactory circuits in drosophilids. Neuron *93*, 661–676.e6.

Quinlan, A.R., and Hall, I.M. (2010). BEDTools: a flexible suite of utilities for comparing genomic features. Bioinformatics *26*, 841–842.

Rosenbloom, K.R., Armstrong, J., Barber, G.P., Casper, J., Clawson, H., Diekhans, M., Dreszer, T.R., Fujita, P.A., Guruvadoo, L., Haeussler, M., et al. (2015). The UCSC Genome Browser database: 2015 update. Nucleic Acids Res. *43*, D670–D681.

Ryner, L.C., Goodwin, S.F., Castrillon, D.H., Anand, A., Villella, A., Baker, B.S., Hall, J.C., Taylor, B.J., and Wasserman, S.A. (1996). Control of male sexual behavior and sexual orientation in Drosophila by the fruitless gene. Cell *87*, 1079–1089.

Savarit, F., Sureau, G., Cobb, M., and Ferveur, J.F. (1999). Genetic elimination of known pheromones reveals the fundamental chemical bases of mating and isolation in Drosophila. Proc. Natl. Acad. Sci. U S A *96*, 9015–9020.

Scott, K., Brady, R., Jr., Cravchik, A., Morozov, P., Rzhetsky, A., Zuker, C., and Axel, R. (2001). A chemosensory gene family encoding candidate gustatory and olfactory receptors in Drosophila. Cell *104*, 661–673.

Seeholzer, L.F., Seppo, M., Stern, D.L., and Ruta, V. (2018). Evolution of a central neural circuit underlies Drosophila mate preferences. Nature *559*, 564–569.

Siepel, A., Bejerano, G., Pedersen, J.S., Hinrichs, A.S., Hou, M., Rosenbloom, K., Clawson, H., Spieth, J., Hillier, L.W., Richards, S., et al. (2005). Evolutionarily conserved elements in vertebrate, insect, worm, and yeast genomes. Genome Res. *15*, 1034–1050.

Spieth, H.T. (1952). Mating behavior within the genus Drosophila (Diptera). Bull. Am. Mus. Nat. Hist. *99*, 395–474.

Spieth, H.T. (1974). Courtship behavior in Drosophila. Annu. Rev. Entomol. *19*, 385–405.

Starostina, E., Liu, T., Vijayan, V., Zheng, Z., Siwicki, K.K., and Pikielny, C.W. (2012). A Drosophila DEG/ENaC subunit functions specifically in gustatory neurons required for male courtship behavior. J. Neurosci. *32*, 4665–4674.

Stern, D.L., Crocker, J., Ding, Y., Frankel, N., Kappes, G., Kim, E., Kuzmickas, R., Lemire, A., Mast, J.D., and Picard, S. (2017). Genetic and transgenic reagents for *Drosophila simulans*, *D. mauritiana*, *D. yakuba*, *D. santomea*, and *D. virilis*. G3 (Bethesda) *7*, 1339–1347.

Sturtevant, A. (1919). A new species closely resembling Drosphila melanogaster. Psyche (Stuttg.) *26*, 153–155.

Sturtevant, A.H. (1920). Genetic studies on Drosophila simulans. I. Introduction. Hybrids with Drosophila melanogaster. Genetics *5*, 488–500.

Tamura, K., Subramanian, S., and Kumar, S. (2004). Temporal patterns of fruit fly (Drosophila) evolution revealed by mutation clocks. Mol. Biol. Evol. *21*, 36–44.

Tanimura, T., Isono, K., Takamura, T., and Shimada, I. (1982). Genetic dimorphism in the taste sensitivity to trehalose inDrosophila melanogaster. J. Comp. Physiol. A Neuroethol. Sens. Neural Behav. Physiol. *147*, 433–437.

R Core Team (2017). R: A language and environment for statistical computing (R Foundation for Statistical Computing).

Thistle, R., Cameron, P., Ghorayshi, A., Dennison, L., and Scott, K. (2012). Contact chemoreceptors mediate male-male repulsion and male-female attraction during Drosophila courtship. Cell *149*, 1140–1151.

Thorne, N., Chromey, C., Bray, S., and Amrein, H. (2004). Taste perception and coding in Drosophila. Curr. Biol. *14*, 1065–1079.

Tootoonian, S., Coen, P., Kawai, R., and Murthy, M. (2012). Neural representations of courtship song in the Drosophila brain. J. Neurosci. *32*, 787–798.

Tusnády, G.E., and Simon, I. (1998). Principles governing amino acid composition of integral membrane proteins: application to topology prediction. J. Mol. Biol. *283*, 489–506.

Tusnády, G.E., and Simon, I. (2001). The HMMTOP transmembrane topology prediction server. Bioinformatics *17*, 849–850.

Vijayan, V., Thistle, R., Liu, T., Starostina, E., and Pikielny, C.W. (2014). Drosophila pheromone-sensing neurons expressing the ppk25 ion channel subunit stimulate male courtship and female receptivity. PLoS Genet. *10*, e1004238.

Wang, Z., Singhvi, A., Kong, P., and Scott, K. (2004). Taste representations in the Drosophila brain. Cell *117*, 981–991.

Wang, L., Han, X., Mehren, J., Hiroi, M., Billeter, J.-C., Miyamoto, T., Amrein, H., Levine, J.D., and Anderson, D.J. (2011). Hierarchical chemosensory regulation of male-male social interactions in Drosophila. Nat. Neurosci. *14*, 757–762.

Weber, J.N., Peterson, B.K., and Hoekstra, H.E. (2013). Discrete genetic modules are responsible for complex burrow evolution in Peromyscus mice. Nature *493*, 402–405.

Weiss, L.A., Dahanukar, A., Kwon, J.Y., Banerjee, D., and Carlson, J.R. (2011). The molecular and cellular basis of bitter taste in Drosophila. Neuron *69*, 258–272.

Wisotsky, Z., Medina, A., Freeman, E., and Dahanukar, A. (2011). Evolutionary differences in food preference rely on Gr64e, a receptor for glycerol. Nat. Neurosci. *14*, 1534–1541.

Wu, M.V., Manoli, D.S., Fraser, E.J., Coats, J.K., Tollkuhn, J., Honda, S., Harada, N., and Shah, N.M. (2009). Estrogen masculinizes neural pathways and sex-specific behaviors. Cell *139*, 61–72.

Xie, Y. (2016). knitr: a general-purpose package for dynamic report generation in R. https://cran.r-project.org/web/packages/knitr/index.html.

Xu, X., Coats, J.K., Yang, C.F., Wang, A., Ahmed, O.M., Alvarado, M., Izumi, T., and Shah, N.M. (2012). Modular genetic control of sexually dimorphic behaviors. Cell *148*, 596–607.

Yamamoto, D., and Koganezawa, M. (2013). Genes and circuits of courtship behaviour in Drosophila males. Nat. Rev. Neurosci. *14*, 681–692.

Zhu, X., Xu, Y., Yu, S., Lu, L., Ding, M., Cheng, J., Song, G., Gao, X., Yao, L., Fan, D., et al. (2014). An efficient genotyping method for genome-modified animals and human cells generated with CRISPR/Cas9 system. Sci. Rep. *4*, 6420.

STAR★METHODS

KEY RESOURCES TABLE

REAGENT or RESOURCE	SOURCE	IDENTIFIER
Chemicals, Peptides, and Recombinant Proteins		
Quinine-HCl	SigmaAldrich	CAS: 6119-47-7
Sucrose	JT Baker	CAS: 57-50-1
Brilliant blue FCF	Wako Pure Chemical	CAS: 3844-45-9
Sulforhodamine	SigmaAldrich	CAS: 3520-42-1
Critical Commercial Assays		
SuperScript III First-Strand Synthesis	Invitrogen, ThermoFisher	Cat # 18080051
Experimental Models: Organisms/Strains		
D. simulans: wildtype	Drosophila Species Stock Center (University of California, San Diego)	14021-0251.001
D. simulans: w^{501}	Drosophila Species Stock Center (University of California, San Diego)	14021-0251.195
D. yakuba: wildtype	Drosophila Species Stock Center (University of California, San Diego)	14021-0261.00
D. virilis: wildtype	Drosophila Species Stock Center (University of California, San Diego)	15010-1051.00
D. melanogaster: Canton-S	Bloomington Drosophila Stock Center	RRID:BDSC_64349,
D. simulans: $Gr32a^{\Delta 10}$	This paper	N/A
D. simulans: $Gr32a^{\Delta 26}$	This paper	N/A
D. simulans: $Gr32a^{\Delta 141}$	This paper	N/A
D. simulans: $Gr33a^{\Delta 10}$	This paper	N/A
D. simulans: $Gr33a^{\Delta 96}$	This paper	N/A
D. simulans: $Ppk25^{+2}$	This paper	N/A
D. simulans: $Ppk25^{\Delta 4}$	This paper	N/A
D. simulans: UAS-ReaChR::Citrine.sim986	This paper	N/A
D. melanogaster: UAS-ReaChR:: Citrine.VK05	Bloomington Drosophila Stock Center	RRID:BDSC_53749
D. simulans: Gr32a^sim^-GAL4.sim986	This paper	N/A
D. simulans: Gr32a^mel^-GAL4.sim986	This paper	N/A
D. melanogaster: Gr32a^sim^-GAL4.attP2	This paper	N/A
D. melanogaster: Gr32a^mel^-GAL4.attP2	This paper	N/A
Oligonucleotides		
Primers: Amplifying Gr32a Regulatory Region	See Table S1	N/A
CRISPR oligos: Targeting *D. simulans* Gr32a	See Table S1	N/A
CRISPR oligos: Targeting *D. simulans* Gr33a	See Table S1	N/A
CRISPR oligos: Targeting *D. simulans* Ppk25	See Table S1	N/A
Primers: RT-PCR of *D. simulans* Gr32a, Gr33a, Ppk25, and tubulin	See Table S1	N/A
Recombinant DNA		
pJFRC2(UAS-ReaChR::Citrine)	Inagaki et al., 2014	N/A
pBPGw	Pfeiffer et al., 2008	RRID: Addgene_17574
pDCC6	Gokcezade et al., 2014	RRID: Addgene_59985

(*Continued on next page*)

Continued

REAGENT or RESOURCE	SOURCE	IDENTIFIER
Software and Algorithms		
ImageJ	NIH	https://imagej.nih.gov/ij/index.html; RRID: SCR_003070
MATLAB	MathWorks	https://www.mathworks.com/products.html; RRID: SCR_001622
ProtScale: Kyte and Doolittle hydrophobicity scale	Artimo et al., 2012	https://web.expasy.org/protscale/
HMMTOP	Tusnády and Simon, 1998, 2001	http://www.enzim.hu/hmmtop/
UCSC Genome Browser, 2015 update	Blanchette et al., 2004; Karolchik et al., 2004; Rosenbloom et al., 2015	https://genome.ucsc.edu/cgi-bin/hgTracks?db=dm6&position=chr2L%3A11110412-11114209; RRID:SCR_005780
phyloP	Pollard et al., 2010; Siepel et al., 2005	https://github.com/CshlSiepelLab/phast; http://compgen.cshl.edu/phast/background.php
bedops	Neph et al., 2012	https://bedops.readthedocs.io/; RRID:SCR_012865
bedtools	Quinlan and Hall, 2010	https://github.com/arq5x/bedtools2; RRID:SCR_006646
R	Comprehensive R Archive Network (CRAN)	https://cran.r-project.org/; RRID:SCR_003005
R, Python and shell script code	See STAR Methods: Tests for non-neutral evolution	https://github.com/aavilaherrera/flymating
CRAN: tidyverse	Comprehensive R Archive Network (CRAN)	https://cran.r-project.org/package=tidyverse
CRAN: rmarkdown	Comprehensive R Archive Network (CRAN)	https://cran.r-project.org/package=rmarkdown
CRAN: knitr	Comprehensive R Archive Network (CRAN)	https://cran.r-project.org/package=knitr
CRAN: kableExtra	Comprehensive R Archive Network (CRAN)	https://cran.r-project.org/package=kableExtra

CONTACT FOR REAGENT AND RESOURCE SHARING

Further information and requests for resources and reagents should be directed to and will be fulfilled by the Lead Contact, Nirao Shah (nirao@stanford.edu).

EXPERIMENTAL MODEL AND SUBJECT DETAILS

D. simulans (14021-0251.001), w[501] *D. simulans* (14021-0251.195), *D. yakuba* (14021-0261.00), and *D. virilis* (15010-1051.00) were obtained from the *Drosophila* Species Stock Center at the University of California, San Diego. WT *D. melanogaster* were in the Canton-S background. *D. melanogaster* UAS-ReaChR::Citrine.VK05 was obtained from the Bloomington *Drosophila* Stock Center (#53749). Transgenic and CRISPR-mediated mutant flies were generated as described below.

METHOD DETAILS

Generating D. simulans Gr32a, Gr33a, or Ppk25 mutants

CRISPR guides were chosen from a list generated by flyCRISPR Optimal Target Finder (flycrispr.molbio.wisc.edu/tools). We targeted exon 1 of *D. simulans Gr32a* and *Ppk25*, and exon 2 of *Gr33a*. CRISPR oligos were annealed and ligated to plasmid pDCC6 {Addgene # 59985, (Gokcezade et al., 2014)} following restriction digest with *BbsI*. Sequences used to synthesize CRISPR oligos are provided in Table S1. Plasmids were injected at 100 ng/uL concentrations for each of 2 - 3 plasmids targeting a single gene. Animals were screened for mutations by PCR followed by 15% non-denaturing PAGE (Zhu et al., 2014) or directly by sequencing. Please see Table S3 for details on results of CRISPR injections for *D. simulans*. All CRISPR-generated mutant strains were backcrossed at least 5 times

to WT *D. simulans* before testing for behavior in order to minimize effects of off-target mutations on phenotypes under study. Subsequent to this out-crossing to WT *D. simulans*, we mated heterozygous flies to obtain homozygous stocks for each allele. Given the absence of balancers in *D. simulans*, we verified genotypes at each generation by PCR analysis to generate homozygous stocks.

Generating D. simulans and *D. melanogaster* transgenic animals

To make Gr32a-GAL4 lines, we amplified the ~3.8 kb region upstream of the Gr32a start codon from *D. simulans* or *D. melanogaster* (primer sequences provided in Table S1) and subcloned it into pENTR/TOPO plasmid followed by Gateway-mediated subcloning into pBPGw. We then phiC31-integrated each DNA construct into Chr III landing sites for each species, sim986 for *D. simulans* and attp2 for *D. melanogaster* (Groth et al., 2004; Knapp et al., 2015; Pfeiffer et al., 2010; Stern et al., 2017). pJFRC2(10xUAS-ReaChR::Citrine) plasmid (Inagaki et al., 2014) was provided by David Anderson, and it was used to generate the Citrine reporter in *D. simulans* using the landing site described above. Embryo injections were performed by Rainbow Transgenics (Camarillo, CA) or BestGene (Chino Hills, CA).

Molecular analysis of Gr32a, Gr33a, and Ppk25 mutations in D. simulans

RNA was isolated from 10 WT or mutant *D. simulans* males (Trizol, ThermoFisher) and converted to cDNA using SuperScript III First-Strand Synthesis (Invitrogen, ThermoFisher). RT-PCR was performed using primers based on coding sequence (Table S1) that spanned exon-intron junctions of the respective locus (*Gr32a*, *Gr33a*, or *Ppk25*) to avoid amplifying products from genomic DNA. Use of these primers did not generate detectable product in no-RT controls. We subcloned and sequenced RT-PCR products from flies mutant for each allele of *Gr32a*, *Gr33a*, and *Ppk25*; we also directly sequenced RT-PCR products from flies mutant for each allele of *Gr32a* (except *Gr32a*[J26]), *Gr33a*, and *Ppk25*. RNA isolation and the subsequent RT-PCR and sequencing were performed on 2-3 independent cohorts of WT and mutant flies. Sequence reads of subclones obtained from these RT-PCR studies and their alignment to the corresponding WT allele confirmed the presence of the expected mutation for each fly stock.

Histology

Tarsi were dissected in ice-cold PBS, fixed in fresh 4% paraformaldehyde at 22°C, washed 3x in PBT, and then mounted as described before (Fan et al., 2013). Samples were imaged using a Zeiss LSM700 (Z stacks) and processed in ImageJ.

Courtship assays

All courtship assays were performed at zeitgeber time 6-10 at 22°C, illuminated by a fluorescent ring lamp (22W) suspended 4 cm above the courtship chamber and recorded with a Sony camcorder (HDR-XR550V) (Fan et al., 2013). Experiments performed under dark conditions were illuminated by red LEDs and recorded as above in a dark room. Virgin flies were collected at eclosion and light entrained (12 hours L/D, 25C) for 5-7 days prior to testing. Experimental males were kept in isolation and tested with flies that were group-housed (~20 flies per vial) by species and sex. Foreleg tarsi were surgically removed at eclosion and males were tested as described above. We used w[501] *D. simulans* as targets in male-male assays to distinguish them by eye color from test males. Behavioral assays were scored blind to genotype, using the MATLAB software ScoreVideo (Wu et al., 2009). We scored courtship as the period of time male flies spent chasing the stimulus fly, performing unilateral wing extension (courtship song), licking, abdominal bending (attempted copulation), or copulation. Courtship Index (CI) was calculated as the time spent by the male performing these behaviors, divided by the total assay time (15 minutes).

Taste assay

Preference assays were performed as described previously (Moon et al., 2009). 60-well plates were prepared the day prior to experimentation and kept at 4°C. Dyes were diluted from stock solutions (Brilliant blue FCF and Sulforhodamine B, 12.5 mg/ml each) and resuspended in agarose, to which sucrose or sucrose spiked with quinine-HCl were subsequently added. Final concentrations were: agarose (1%), Brilliant blue FCF (0.125 mg/mL; Wako Pure Chemical), Sulforhodamine B (0.125 mg/mL; SigmaAldrich), sucrose (1 mM; JT Baker), and sucrose (5 mM) spiked with quinine (0.5 mM; SigmaAldrich). Substrate with sucrose or sucrose spiked with quinine were randomly colored blue or red and counterbalanced for all experiments. 3-4 day old male and female flies were flipped into fresh food for 2 days at 12-hour light/dark cycle at 25°C. Flies were then food deprived by flipping them into vials containing 1% agarose and placed in the dark for 24 hours. Flies were then briefly anesthetized with CO_2 and loaded onto the 60-well plates (zeitgeber time 2-3), which were placed in the dark at 25°C for 90 min. Abdomens were scored as blue, red, purple (mixed eating), or no food coloring blind to genotype and color condition. A Preference Index was calculated for each 60-well plate as follows: $(N^B + 0.5*N^P)/(N^B + N^R + 0.5*N^P)$ or $(N^R + 0.5*N^P)/(N^B + N^R + N^P)$ where N^B, N^R, and N^P = total # flies with blue, red, and purple abdomens, respectively. Each genotype was tested ≥ 6 times.

Tests for Non-Neutral Evolution

Alignments of genomes from 27 insect species (23 drosophilids, housefly, mosquito, honeybee, and beetle) were generated for coordinates (dm6: chr2L:11,110,412-11,114,209) encompassing the *D. melanogaster* Gr32a ~3.8 kb regulatory sequence, and this alignment was subsequently downloaded from the Table Browser (UCSC Genome Browser, 2015 update) (Blanchette et al., 2004; Karolchik et al., 2004; Rosenbloom et al., 2015). PhyloP scores were computed for this region for three main tests: 1) a

basewise "all-branches" test for conserved or accelerated evolution in all species compared to a neutral model (one test per nucleotide), 2) a whole-region "all-branches" test for conserved evolution in all species compared to a neutral model (one test for the whole region), and 3) a basewise "subtree" test for conserved or accelerated evolution in the designated species (*D. melanogaster* or *D. simulans*) compared to the other species (one test per nucleotide for each designate species) (Pollard et al., 2010). PhyloP scores are negative $\log_{10}$ P values of a likelihood ratio test comparing two evolutionary models (alternate versus neutral or subtree versus subtree complement). Scores near "0" indicate the expected rate of evolution, while large scores indicate conservation (phyloP score > 2) or acceleration (phyloP score < -2). PhyloP scores were tallied across coding sequence, introns, UTRs, and intergenic regions (Siepel et al., 2005). The phylogenetic model for neutral evolution was based on 4-fold degenerate sites in the 27-species genomic alignment and also downloaded from the UCSC Genome Browser. PhyloP scores and R code are made available for reproducible workflow at https://github.com/aavilaherrera/flymating (Allaire et al., 2017; R Core Team, 2017; Xie, 2016) (https://cran.r-project.org/doc/FAQ/R-FAQ.html#Citing-R). This code uses bedtools and bedops (Neph et al., 2012; Quinlan and Hall, 2010).

Hydrophobicity plot

Hydrophobicity scores were generated with ProtScale (Artimo et al., 2012) using *D. melanogaster* or *D. simulans* Gr32a amino acid sequences as input. We used the Kyte and Doolittle hydrophobicity scale with a window size of 19 amino acids and uniform weights across all residues. The seven transmembrane domains were identified using HMMTOP (Tusnády and Simon, 1998, 2001) to predict the topology of Gr32a for both *D. melanogaster* and *D. simulans*.

QUANTIFICATION AND STATISTICAL ANALYSIS

We used Fisher's exact test to analyze categorical data (e.g., percent assays with CI > 0.05) and we used the Bonferroni correction for multiple group comparisons as necessary. For other comparisons, we first tested whether data were normally distributed using a Lillefors' goodness-of-fit test using MATLAB. Data for Figure S1B were analyzed with a Student's t test; data for all other figure panels were tested with a non-parametric test (Kolmogorov-Smirnov test for two groups or Kruskal-Wallis test). A Tukey's post hoc test following multiple group comparisons was used to determine which groups differed significantly.

Supplemental Information

Evolution of Mechanisms that Control

Mating in *Drosophila* Males

Osama M. Ahmed, Aram Avila-Herrera, Khin May Tun, Paula H. Serpa, Justin Peng, Srinivas Parthasarathy, Jon-Michael Knapp, David L. Stern, Graeme W. Davis, Katherine S. Pollard, and Nirao M. Shah

Figure S1, related to Figures 1 and 2

A

D. simulans

D. melanogaster

D. yakuba

D. virilis

40   8 4 0

Divergence Time (million years)

B

x D. yak ♀

Courtship Index (C.I.)

NS

(22) (23)

C.I. > 0.05, Fraction Assays

(22) (23)

D. simulans male:
○ Control
○ No Tarsi

C

□ Corresponding GAL4 alone
▨ Corresponding GAL4 + Gr32a^mel-GAL4

# of Citrine+ Cells

(10) (16)   (15) (17)

Gr32a^mel-GAL4   Gr32a^sim-GAL4

D. mel ♂

D

~3.8 kb Regulatory Region

Gr32a Coding Sequence

mel
sim
sec
yak
ere
bia
suz
ana
bip
eug
ele
kik
tak
rho
fic
pse
per
mir
wil
vir
moj
alb
gri
dom
gab
mlf
cas

27 insects Alignment by Multiz

E

27 insects Conservation by PhastCons

F   **G**   **H**

27 Insects   *D. melanogaster*   *D. simulans*

# of alignment columns

PhyloP score   PhyloP score   PhyloP score

I *x D. sim ♀*   **J** *x D. mel ♀*

Mid-Line Crossings

NS   *

(11) (09)   (10) (10)

D. simulans male:
○ Control
○ No Tarsi

K *D. sim ♂* Gr32a^sim-GAL4

L *D. mel ♂* Gr32a^mel-GAL4

Citrine

SEZ   SEZ

Figure S1: A regulatory region upstream of *Gr32a* coding sequence is conserved across drosophilids. Related to Figures 1 and 2.

(A) Evolutionary relationship of the four *Drosophila* species used in this study.

(B) Foreleg tarsi do not inhibit *D. simulans* males from courting *D. yakuba* females. Mean ± SEM; each circle denotes CI of a *D. simulans* male; n = 22 - 23/cohort; ***p<0.001.

(C) No difference in the number of Citrine+ cells in T4 and T5 foreleg segments of *D. melanogaster* males observed with either Gr32a^{mel}-GAL4 or Gr32a^{sim}-GAL4 alone or in combination. These findings indicate that the upstream regulatory sequence in Gr32a is functionally conserved between *D. melanogaster* and *D. simulans*; however, it is formally possible that the similarity in number of Citrine+ cells in *D. melanogaster* carrying one or both *GAL4* alleles reflects effects of transvection in the presence of both *GAL4* alleles rather than functional conservation. Mean ± SEM; each circle denotes Citrine+ cell count for a foreleg tarsum; n = 10 - 17/genotype.

(D) 27-insect alignment of the ~3.8 kb DNA element that drives *Gr32a* expression in *D. melanogaster* and *D. simulans*. mel, *D. melanogaster* (blue); sim, *D. simulans* (orange); sec, *D. sechellia*; yak, *D. yakuba*; ere, *D. erecta*; bia, *D. biarmipes*; suz, *D. suzukii*; ana, *D. ananassae*; bip, *D. bipectinata*; eug, *D. eugracilis*; ele, *D. elegans*; kik, *D. kikkawai*; tak, *D. takahashii*; rho, *D. rhopaloa*; fic, *D. ficusphila*; pse, *D. pseudoobscura*; per, *D. persimilis*; mir, *D. miranda*; wil, *D. willistoni*; vir, *D. virilis*; moj, *D. mojavensis*; alb, *D. albomicans*; gri, *D. grimshawi*; dom, *Musca domestica*; gab, *Anopheles gambiae*; mlf, *Apis mellifera*; cas, *Tribolium castaneum*.

(E) Track showing PhastCons conservation score across the region in (D). Pink bar indicates the intergenic region directly 5' of the Gr32a start codon and 5'UTR, which contains several blocks of highly conserved sequence. Higher peaks indicate higher likelihood of bases being in a strongly conserved element.

(F) Distribution of nucleotide resolution phyloP conservation scores for the region shown in (D). Most bases in the region are evolving at the same or slower rate than 4-fold degenerate (4D) sites in the multiple sequence alignment of 27 insects. Large positive (> 2) or negative (< -2) scores indicate conservation or acceleration, respectively. Scores near "0" indicate a similar substitution rate to 4D sites.

(G, H) Distribution of phyloP scores for branch-specific evolutionary tests. Most bases in the ~3.8 kb region are likely evolving more slowly or as slowly as expected in *D. melanogaster* (G) and *D. simulans* (H) compared to the other 26 insects in the tree. Scores near "0" indicate a similar rate of DNA evolution in the designated species relative to all other species in the tree.

(I, J) Removing the foreleg tarsi of *D. simulans* males does not diminish locomotor activity during courtship assays. Mean ± SEM; each circle denotes # of midline crossings of a *D. simulans* male; n = 9 - 11/cohort; *p<0.05.

(K, L) Projection pattern of Gr32a neurons in the SEZ is similar between *D. melanogaster* and *D. simulans* males. n = 3 - 4 brains/genotype; scale bar = 50 μm.

Figure S2, related to Figure 3

A

D. simulans Gr32a

B

| | WT | Gr32a$^{\Delta10}$ | Gr32a$^{\Delta26}$ | Gr32a$^{\Delta141}$ |

1650bp — Gr32a

500bp
400bp — tubulin

C

```
         WT   CCGGATGCCCGTGTTAACCCGGGATGCCTTCAGTAGAGATG//GATGCCCATATACGAACAGGTCTCCGACTATG        PAM
       Δ10bp  CCGGATGCCCG----------GGATGCCTTCAGTAGAGATG//GATGCCCATATACGAACAGGTCTCCGACTATG        Protospacer
       Δ26bp  CCGGATGCCCG-------------------------GATG//GATGCCCATATACGAACAGGTCTCCGACTATG
      Δ141bp  CCGGATGCCCG-------------------------//---------------------------ACTATG
                        90                       120      210              230
```

D

```
   WT   MSPNTWVIEMPTQKAQSHPYPRRISPYRMPVLTRDAFSRDAPPMPARSHDHPVFEDIRTI
 Δ10bp  MSPNTWVIEMPTQKAQSHPYPRRISPYRMPGMPSVEMHHLCQRGAMIIPFLRTFAPYCPC
 Δ26bp  MSPNTWVIEMPTQKAQSHPYPRRISPYRMPGCTTYASEEP*
Δ141bp  MSPNTWVIEMPTQKAQSHPYPRRISPYRMP--------------------------
                          20            40            60
```

```
                                                              TM1
   WT   LSVLKASGLMPIYEQVSDYEVGPPTKTNEFYSFFVRGVVHALTIFNVYSLFTPISAQLFF
 Δ10bp  SRPVA*
 Δ26bp
Δ141bp  ------------------DYEVGPPTKTNEFYSFFVRGVVHALTIFNVYSLFTPISAQLFF
                      80            100           120
```

E

x *D. yak* ♀

D. simulans male:

○ Control
○ Gr32a$^{\Delta10}$
○ Gr32a$^{\Delta26}$
○ Gr32a$^{\Delta141}$

F

NH$_2$ — TM1 TM2 TM3 TM4 TM5 TM6 TM7 — COOH

G

— *D. simulans* Gr32a
— *D. melanogaster* Gr32a

Figure S2: Generating Gr32a mutant *D. simulans* via CRISPR/Cas9. Related to Figure 3.

(A) Schematic of *D. simulans Gr32a* locus. Pink arrows, PCR primers; green triangles, CRISPR target sites; black rectangles, exons.

(B) RT-PCR products for Gr32a and tubulin in WT and *Gr32a* mutant *D. simulans*, using PCR primers shown in (A). DNA ladder shown in first lane.

(C) DNA sequence comparison of WT and mutant *Gr32a* alleles. PAM, Protospacer Adjacent Motif.

(D) Predicted amino acid sequence of WT and mutant *D. simulans* Gr32a. The predicted first transmembrane domain (TM1) is highlighted in gray in the WT protein. *, premature stop codon.

(E) No difference in courtship of *D. yakuba* females by WT and *Gr32a* mutant *D. simulans* males. Mean ± SEM; each circle represents CI of a male; n = 17 - 21/genotype.

(F) Predicted location of the seven transmembrane domains (black rectangles) in Gr32a based on plot shown in (G). The NH$_2$ terminal is predicted to be intracellular.

(G) Hydrophobicity plot of *D. simulans* and *D. melanogaster* Gr32a. Predicted transmembrane domains are shown by gray shading.

Please see Table S2.

Figure S3, related to Figure 3

A

D. simulans Gr33a

B

WT   Gr33a^Δ10   Gr33a^Δ96

1000bp
850bp — Gr33a

500bp
400bp — tubulin

C

```
WT      CATTCCACTGAATCGCCAGCAATCGGAAACTAACTT//CTTCTCATAAATCTTACCCACATTATTGGCCTCTG   PAM
Δ10bp   CATTCCACTG----------AATCGGAAACTAACTT//CTTCTCATAAATCTTACCCACATTATTGGCCTCTG   Protospacer
Δ96bp   CATTCCACTGAATCGCCAGC---------------//-----------------------TTGGCCTCTG
                    50              70              140              160
```

PAM
Protospacer

D

```
WT      MIQIMNWFSMVIGLIPLNRQQSETNFILDYAMMCIVPIFYVACYLLINLTHIIGLCFLDSCNSVCKLSSHLFMHLGAFLY
Δ10bp   MIQIMNWFSMVIGLIPLNRKLTSYSTTP*
Δ96bp   MIQIMNWFSMVIGLIPLNRQL----------------------------------GLCFLDSCNSVCKLSSHLFMHLGAFLY
                          20              40              60              80
```

E   x D. sim ♀   x D. mel ♀   x D. yak ♀   x D. vir ♀   **G**   x D. sim ♂

Courtship Index (C.I.)

(20) (24) (20)   (17) (13) (14)   (17) (21) (20)   (10) (10) (12)   (21) (14) (17)

D. simulans male:
○ Control
○ Gr33a^Δ10
○ Gr33a^Δ96

F   **H**

C.I. > 0.05, Fraction Assays

(20) (24) (20)   (17) (13) (14)   (17) (21) (20)   (10) (10) (12)   (21) (14) (17)

I

D. melanogaster — Gr33a ⊣ Quinine Feeding ⊣ ? Gr33a — *D. simulans*

J

Preference Index

***

(10) (6) (10)

D. simulans:
○ Control
○ Gr33a^Δ10
○ Gr33a^Δ96

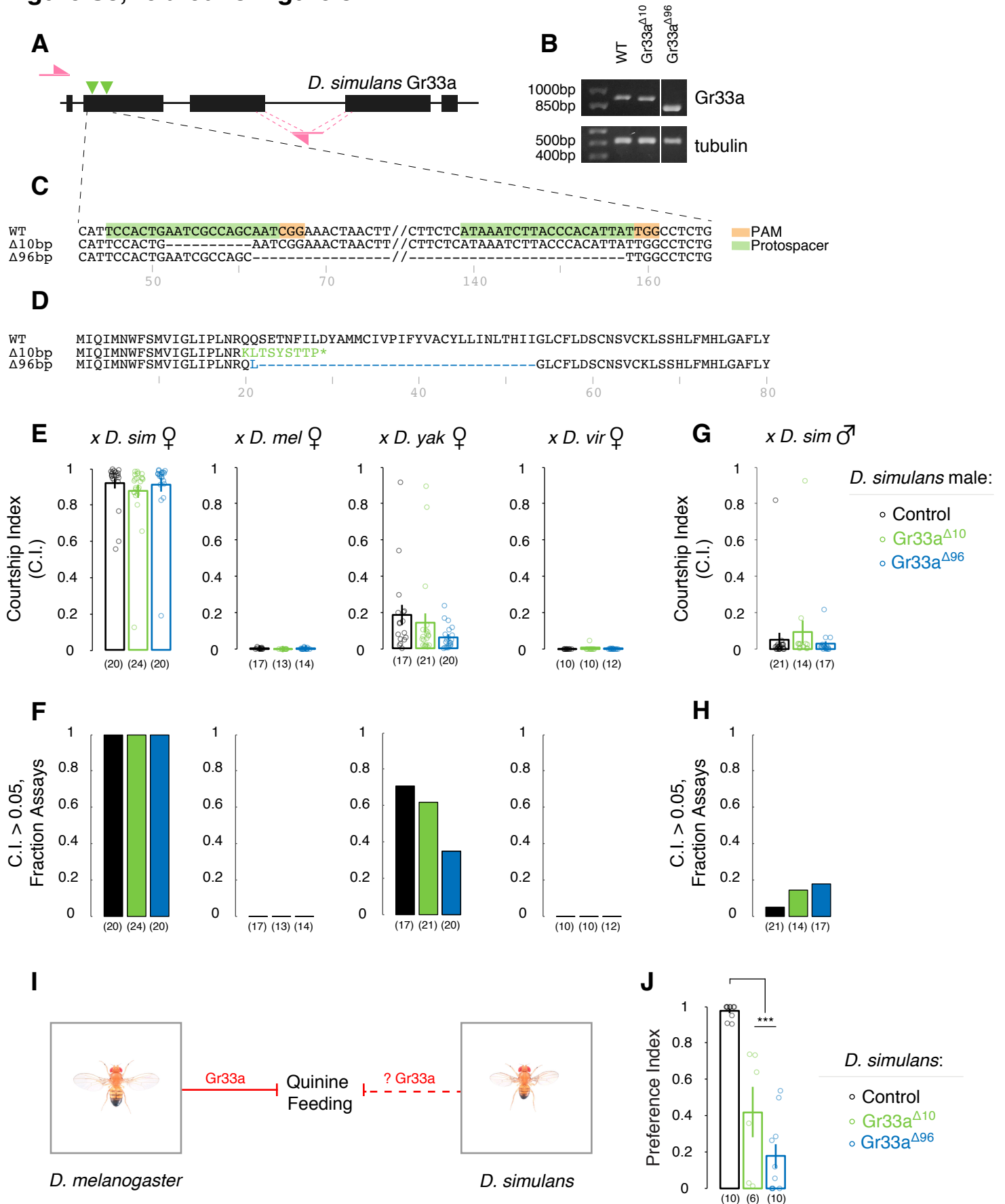**Figure S3: Gr33a is not required to inhibit interspecies courtship behavior of *D. simulans* males but does inhibit *D. simulans* from feeding on quinine. Related to Figure 3.**

(A) Schematic of *D. simulans* Gr33a locus. Pink arrows, PCR primers; green triangles, CRISPR target sites; black rectangles, exons.

(B) RT-PCR products for Gr33a and tubulin in WT and *Gr33a* mutant *D. simulans*, using PCR primers shown in (A). Note that products from WT, $Gr33a^{\Delta10}$ and $Gr33a^{\Delta96}$ flies were run on the same gel, and lane between $Gr33a^{\Delta10}$ and $Gr33a^{\Delta96}$ has been cropped out for clarity of comparison. DNA ladder shown in first lane.

(C) DNA sequence comparison of WT and mutant *Gr33a* alleles.

(D) Predicted amino acid sequence of WT and mutant *D. simulans* Gr33a. *, premature stop codon.

(E, F) WT and *Gr33a* mutant *D. simulans* males court conspecifics at high levels and show similar low (*D. yakuba*) to minimal (*D. melanogaster* and *D. virilis*) levels of courtship toward females of other species.

(G, H) WT and Gr33a mutant *D. simulans* males show similar low levels of courtship toward conspecific males.

Mean ± SEM; each circle denotes CI of one male; n = 10 - 24/genotype.

(I) We tested whether, similar to *D. melanogaster*, Gr33a inhibits feeding on quinine-containing food in *D. simulans*.

(J) Significant decrease in preference by *Gr33a* mutant *D. simulans* for food containing only sucrose.

Mean ± SEM; each circle denotes Preference Index for one experiment; 90 ± 4 *D. simulans* of each genotype were used/experiment; n = 6 - 10 experiments/genotype; ***p<0.001.

Figure S4, related to Figure 4

A

D. simulans ppk25

B

WT Ppk25+2 Ppk25Δ4

650bp
500bp Ppk25

500bp
400bp tubulin

C

```
WT    ATGGAATCCAAAGGGAGTCGGCCGAAGCAACCGGACT//CGGCATGCCCTACATCGCCCGCAAGGATC      PAM
+2bp  ATGGAATCCAAAGGGAGTCGGCCGAAGC[cg]AACCG//CGGCATGCCCTACATCGCCCGCAAGGATC      Protospacer
Δ4bp  ATGGAATCCAAAGGGAGTCGGCCGAAGCAACCGGACT//CGGCATGCCCTACATCGC----AAGGATC
                    10            30              80                100
```

D

```
WT    MESKGSRPKQPDWLAEVCQESSIHGMPYIARKDLHWTERILWALIILGSAYYAISSCLNQWYRFRDNPLVYEYEYLFGLR
+2bp  MESKGSRPKPNRTGSPRCARSPPSTACPTSPARISTGPSASCGH*
Δ4bp  MESKGSRPKQPDWLAEVCQESSIHGMPYIARISTGPSASCGH*
               20          40              60              80
```

D. sim ♂ x D. sim ♀   *D. mel ♂ x D. mel ♀*

E

*** Courtship Index (C.I.)

** C.I. > 0.05, Fraction Assays

(12) (20)   (12) (20)

F

*** Courtship Index (C.I.)

C.I. > 0.05, Fraction Assays

(12) (22)   (12) (22)

○ Fluorescent Light
○ Red Light

G

x D. sim ♀ (In Dark)   *x D. mel ♀ (In Dark)*

*** Courtship Index

(09) (08)   (07) (11)

D. simulans male:
○ Control
○ No Tarsi

H

x D. mel ♀   *x D. yak ♀*   *x D. vir ♀*

Courtship Index (C.I.)

**

(14) (20) (20)   (18) (21) (24)   (6) (9) (12)

D. simulans male:
○ Control
○ Ppk25+2
○ Ppk25Δ4

I

C.I. > 0.05, Fraction Assays

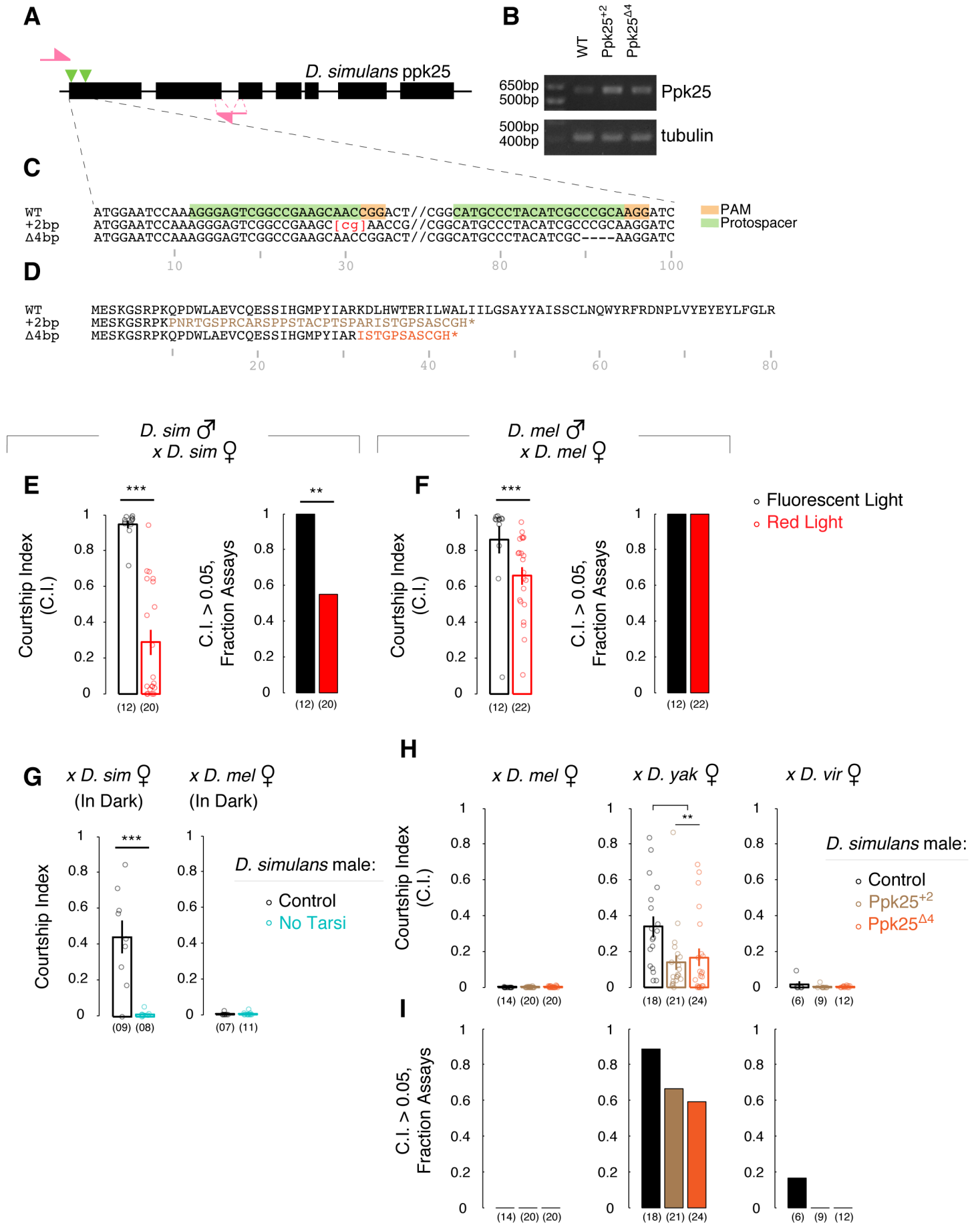(14) (20) (20)   (18) (21) (24)   (6) (9) (12)

Figure S4: Ppk25 is not essential to inhibit interspecies courtship by *D. simulans* males. Related to Figure 4.

(A) Schematic of *D. simulans Ppk25* locus. Pink arrows, PCR primers; green triangles, CRISPR target sites; black rectangles, exons.

(B) RT-PCR products for Ppk25 and tubulin in WT and *Ppk25* mutant *D. simulans*, using PCR primers shown in (A). DNA ladder shown in first lane.

(C) DNA sequence comparison of WT and mutant *Ppk25* alleles.

(D) Predicted amino acid sequence of WT and mutant *D. simulans* Ppk25. *, premature stop codon.

(E, F) *D. simulans* and *D. melanogaster* males court conspecific females less under red light-only illumination.

(G) *D. simulans* males require foreleg tarsi for courtship under dark conditions.

(H, I) No difference between *D. simulans* males WT or mutant for Ppk25 in courtship of *D. melanogaster* and *D. virilis* females. Mutant males court *D. yakuba* females less than WT (G). Mean ± SEM; each circle denotes CI for one male; n = 6-24/cohort; **p<0.01; ***p<0.001.

Table S1. Related to Figures 2, S2, S3, and S4

Name	Experiment	5' to 3' Sequence
sim32 fwd	Amplifying ~3.8kb Gr32a regulatory region from *D. simulans* to generate Gr32a^{sim}-GAL4	GTCCCCTTGCGGTTGTTCT
sim32 rev		TTCAATTACCCAAGTGTTCG
mel32 fwd	Amplifying ~3.8kb Gr32a regulatory region from *D. melanogaster* to generate Gr32a^{mel}-GAL4	AAGTGGTTGGTCTTGGAT
mel32 rev		TTCAATTACCCAAGTGTTCG
CrisprGr32a A fwd	CRISPR oligos targeting *D. simulans* Gr32a	CTTCGGAAGGCATCCCGGGTTAACA
CrisprGr32a A rev		AAACTGTTAACCCGGGATGCCTTCC
CrisprGr32a B fwd		CTTCGTCGGAGACCTGTTCGTATAT
CrisprGr32a B rev		AAACATATACGAACAGGTCTCCGAC
CrisprGr32a C fwd		CTTCGTTTTACTCGTTCTTCGTAAG
CrisprGr32a C rev		AAACCTTACGAAGAACGAGTAAAAC
CrisprGr33a A fwd	CRISPR oligos targeting *D. simulans* Gr33a	CTTCGTCCACTGAATCGCCAGCAAT
CrisprGr33a A rev		AAACATTGCTGGCGATTCAGTGGAC
CrisprGr33a B fwd		CTTCGATAAATCTTACCCACATTAT
CrisprGr33a B rev		AAACATAATGTGGGTAAGATTTATC
CrisprGr33a C fwd		CTTCGGCTGAGTCTTTATCGCCGAA
CrisprGr33a C rev		AAACTTCGGCGATAAAGACTCAGCC
CrisprPpk25 A fwd	CRISPR oligos targeting *D. simulans* Ppk25	CTTCGAGGGAGTCGGCCGAAGCAAC
CrisprPpk25 A rev		AAACGTTGCTTCGGCCGACTCCCTC
CrisprPpk25 B fwd		CTTCGCATGCCCTACATCGCCCGCA
CrisprPpk25 B rev		AAACTGCGGGCGATGTAGGGCATGC
Gr32a RTPCR fwd	primers for RT-PCR of *D. simulans* Gr32a	TAATCCACAATGCCAAGCAA
Gr32a RTPCR rev		AGGAACTTATCGATGATATTCTGAT
Gr33a RTPCR fwd	primers for RT-PCR of *D. simulans* Gr33a	CGGAGTAGCGAGTAAATTCCA
Gr33a RTPCR rev		TCGGATGTGTTTCCGGTATT
Ppk25 RTPCR fwd	primers for RT-PCR of *D. simulans* Ppk25	ACATCATGGAATCCAAAGG
Ppk25 RTPCR rev		ATCCAGTGTTTCTAGTTTGCC

tubulin RTPCR fwd	primers for RT-PCR of *D. simulans* tubulin	CTTGTCGCGTGTGAAACACT
tubulin RTPCR rev		GGATCCTGTCCAGAACCAGA

Table S1: List of oligos and primers used in this study. Related to Figures 2, S2, S3, and S4.

Table S2. Related to STAR Methods and Figure S2

Predicted TM domains	Gr32a Amino Acid Range	
	D. melanogaster	*D. simulans*
TM1	101-119	101-120
TM2	134-156	131-149
TM3	187-206	187-206
TM4	215-239	215-239
TM5	310-329	310-327
TM6	356-378	354-378
TM7	419-443	419-443
TM, transmembrane		

Table S2: Predicted transmembrane domains of Gr32a. Related to STAR Methods and Figure S2.

Table S3. Related to STAR Methods and Figures S2, S3, and S4.

Locus	# CRISPR Guides Injected	# injected embryos	# larvae	# G0 flies	# G0 flies that yielded progeny (F1)	# G0 flies that yielded mutant F1 flies	# F1 flies bearing distinct indel mutations	Homozygous Stocks used in study
Gr32a	3	300	40	15	7	3	7	3
	2	300	15	10	5	1	3	0
Gr33a	3	519	298	78	26	3	7	2
Ppk25	2	510	185	86	44	2	4	2

Table S3: *D. simulans* pDCC6 CRISPR injection counts. Related to STAR Methods and Figures S2, S3, and S4.